Received: 17 May 2017 | Accepted: 26 July 2017

DOI: 10.1111/jace.15108

FEATURE ARTICLE

Journal of the American Ceramic Society

The fracture toughness of inorganic glasses

Tanguy Rouxel[1] | **Satoshi Yoshida**[2]

[1]Glass and Mechanics Department, Physics Institute, UMR UR1-CNRS 6251, University of Rennes 1, Rennes Cedex, France

[2]Department of Materials Science, The University of Shiga Prefecture, Hikone, Shiga, Japan

Correspondence
Tanguy Rouxel, Glass and Mechanics Department, Physics Institute, UMR UR1-CNRS 6251, University of Rennes 1, Campus de Beaulieu, 35042 Rennes Cedex, France.
Email: tanguy.rouxel@univ-rennes1.fr

Funding information
FP7 Ideas: European Research Council, Grant/Award Number: 320506 (DAMREG); European Research Council, Grant/Award Number: 320506; JSPS KAKENHI, Grant/Award Number: 15H04124, 16K06730

Abstract

Measuring the fracture toughness (K_{Ic}) of glasses still remains a difficult task, raising experimental and theoretical problems as well. The available methods to estimate K_{Ic} are reviewed, with emphasis on their respective advantages and drawbacks. In view of our current understanding, this analysis gives precedence to the SEPB method. The ultimate glass strength, the critical flaw size, and the indentation load for the onset of crack initiation are discussed, in the light of the fundamentals of fracture mechanics and classical background regarding the mechanics of brittle materials. Analytical expressions were further proposed to predict the fracture energy and fracture toughness of glasses from different chemical systems from their nominal compositions. The theoretical values were compared with the experimental ones, as obtained by self-consistent methods when available. The agreement observed in most cases suggests that measured K_{Ic} values correspond to the crack propagation regime (as opposed to the crack initiation threshold), and supports previous investigations in glasses and ceramics, which showed that a crack tip is nearly atomically sharp in these materials (but for metallic glasses). Some ideas to design tougher glasses are finally presented.

KEYWORDS

cracks/cracking, elastic materials/properties, fracture mechanics/toughness, glass, indentation

1 | INTRODUCTION

Fracture toughness defines the resistance of a material to the extension of a pre-existing flaw (crack). The opening mode being the most critical for brittle materials it is mostly referred to as K_{Ic}, i.e. the critical value of the stress intensity factor for a crack opening normal to its mean propagating plane (mode I). It is an important material characteristics allowing for the estimation of the flaw size from the actual resistance or conversely for the estimation of the practical fracture stress knowing the critical flaw characteristics (size, shape, orientation, and location). A value smaller than 2 MPa.$\sqrt{m}$ is an indication of brittleness and is common for ionocovalent glasses (oxides, chalcogenides, oxycarbonitride). Nevertheless, a glance at Figure 1 reveals that a wide range of values were reported for glasses, from about 0.1 to over 20, depending on the chemical system, and on the composition within a given system as well. Although some correlation were seen between K_{Ic} and Poisson's ratio (ν) when some peculiar class of glass is under scrutiny, there is no one to one trend. Interestingly the softer isn't always the tougher: there are very brittle glasses exhibiting a remarkably low hardness, such as chalcogenide glasses, and vice-versa hard glasses, such as silicon oxynitride ones, being also relatively tough. An even larger spectrum is achieved by playing on the nano-micro-structural features by phase separation or crystallization treatments to meet glass-ceramic materials. It is noteworthy in this latter case that a toughness improvement is not always observed because of the development of residual stresses upon cooling from the heat-treatment temperature, which is of paramount importance to understand the behavior of the final product.

The way to assess brittleness in a quantitative manner is still a matter of controversy and debates. On the one side, inherent brittleness is a very unfavorable situation to

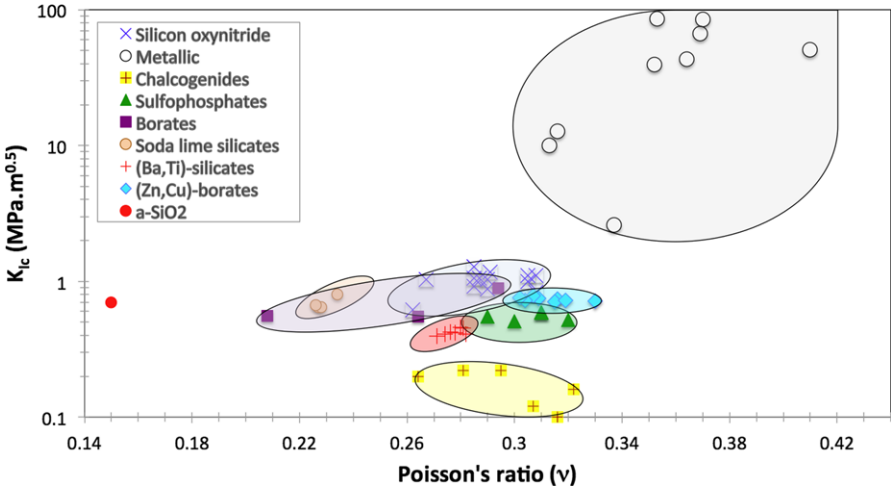

FIGURE 1 The apparent fracture toughness of glasses, as obtained by means of various experimental methods as a function of Poisson's ratio

implement suitable experimental methods and to machine specimens for fracture toughness determination. On the other side, the critical load (P_c) for the initiation of damage (cracks, chips) at the surface under sharp contact loading (indentation, scratching, etc.) is at least as important as fracture toughness. As long as the problem of mechanical surface damage (impact, indentation, scratches) and the consequences on the sructural integrity and on the optical properties are considered, the relevance of K_{Ic} as a key parameter is questionable. Indeed, P_c as well as the geometrical characteristics of the microcracking pattern, which depends on the way the glass deforms under contact loading seem equally essential. A brittleness parameter ($B = H/K_{Ic}$, where H is hardness) was introduced about four decades ago to describe the sensitivity to indentation cracking by comparing the indentation size with the resulting crack length.[1] Nevertheless, as we will show in this paper, correlation between P_c, K_{Ic}, and other materials characteristics such as hardness and elastic moduli still remain to be established. A major problem so far lies in the insufficient understanding of the underlying physics, especially for the inelastic deformation processes, which are responsible for the formation of imprints and scratches. Progress in this area is discussed in this article.

Another issue with fracture toughness, which was already recognized more than a century ago[2] and drove much attention since the 1950', is the environmental effects, and more specifically the effect of humidity. Water in the ambience not only enhances crack extension but also affects crack tips and surface flaws in different ways depending on the composition, and can be either detrimental or advantageous. For instance water penetrating the surface of amorphous silica induces compressive internal stresses that decrease the surface flaw sensitivity. The environmental effects were widely documented and review papers were recently published on this subject.[3] Such effects are thus not further discussed in the present paper. Besides, the domain of surface treatments (thermal and chemical tempering, grinding and polishing, coatings etc.), which are known to significantly affect the crack resistance, and became a very important field of activity both in academic institutions and in the glass industry, is going far beyond the scope of the present analysis and is not considered here.

2 | EXPERIMENTAL METHODS FOR THE DETERMINATION OF FRACTURE TOUGHNESS OF GLASS

The critical stress intensity factor in the crack opening mode (K_{Ic}), refereed to toughness is mostly determined by means of the following expression.[4]

$$K_{Ic} \propto \sigma_r \sqrt{a} \ (\propto: \text{proportional}) \qquad (1)$$

where σ_r is the actual fracture stress of a sample with a pre-existing flaw of length a (critical crack size). The proportionality constant in Equation (1) varies with loading configuration and with the specimen and crack geometries.

There are numerous methods to evaluate fracture toughness and the crack extension behavior, among which only a few were popularized or adapted to glass by glass scientists. Table 1 summarizes some of these methods.[5-36] Indentation-based methods (IF for Indentation Fracture), based on the length of cracks propagating from an indent, or on the critical load to extend a sharp surface flaw, are by far the most common, but needs to be calibrated. Then some self-consistent methods, which are based on the determination of the peak load at fracture of a specimen with a controlled flaw (pre-crack or notch), include the controlled surface flaw (CSF), the single-edge notch beam (SENB), the single-edge precrack beam (SEPB), and the chevron notch beam (CN) methods. In the latter cases, stable crack extension might be observed provided the specimen geometry is carefully designed and the testing

TABLE 1 Measurement methods of fracture toughness of glass

Method	Suitability for glass	Advantages	Drawbacks	References
IF (Indentation Fracture)	Use with care	i Applicable to small specimens. ii Simple testing procedure. iii Suitable to study surface damage and the onset of crack initiation	i Difficulty to identify the crack system. (Half-Penny[7,8,16] or Palmqvist[9-11]) ii Densification affects the value. iii Inapplicable to most glasses. (The method using the Cone-crack length is proposed.)[15]	[5-16]
CSF (Controlled Surface Flaw) IS (Indentation Strength)	Use with care	Easy pre-cracking by indentation	i Residual stress around the indent affects the value. ii Lateral and/or other cracks affect the stress field.	[17–20] (CSF) [21] (IS)
SENB (Single-Edge Notched Beam)	Use with care	Self-consistent	The notch width affects the value	[22, 23]
SEPB (Single-Edge Pre-Cracked Beam)	Suitable	i Self-consistent. ii Tip radius of pre-crack is atomically sharp	Sometimes difficult to obtain and to measure the length of the pre-crack	[16, 17, 24, 25]
CN (Chevron-Notched Beam)	Suitable	i Self-consistent ii Fracture origin is always at the tip of chevron	Machining of the chevron-notch is difficult	[17, 26–28]
DCDC (Double Cleavage Drilled Compression)	Applicable	i Self-consistent. ii Simple loading condition.	i The condition "free from fatigue" is required. (cf. Inert condition or high crack velocity) ii The stress intensity factor at the crack tip isn't precisely known	[29, 30]
CTOD (Crack Tip Opening Displacement)	Applicable	i Self-consistent. ii Useful for bulk metallic glass.	AFM, SEM or TEM observation of the crack-tip is required for oxide glasses.[28]	[31, 32]
DCC (Double Cantilever Cleavage) WOL-type CT (Wedge-Opening-Loading-type Compact Tension)	Applicable	i Self-consistent. ii Simple determination of stress intensity factor	Difficult to machine a specimen	[22, 33, 34] (DCC) [35] (WOL)
DT (Double Torsion)	Applicable	i Self-consistent. ii Simple loading condition. iii Stress intensity factor is independent of the crack length.	The crack propagation occurs not only in the mode I but in the mixed I/III mode	[36]

machine (including the set-up) compliance is small enough. In such circumstance, K_{Ic} can be determined either from the peak load and the corresponding crack length (from Equation 1) or from the mechanical energy dissipated for the complete stable fracture process, namely the work of fracture (WOF = $\int_o^{u_f} P du = 2\gamma S$, where u_f is the specimen displacement at complete fracture, P the applied load, S the overall newly created surface area, and γ the fracture surface energy). The stress-energy similarity principle provides the following expression for K_{Ic}:

$$K_{Ic} = \sqrt{\frac{2\gamma E}{1-\nu^2}} \quad (2)$$

where E is Young's modulus.

It is noteworthy that as temperature is increased, or as the glass transition temperature (T_g) is decreased, or as the interatomic bonding becomes weaker (from iono-covalent to metallic for instance), the stress-strain curve shows some departure from linearity and the validity of the fracture toughness test is questioned. This happens for example in chalcogen-rich chalcogenide glasses as T_g get closer to room temperature, or as glass specimen are heated close to T_g, so that some visco-elasto-plastic behavior is observed, which ultimately results in the brittle-to-ductile transition. In the case of metallic glasses, some plastic zone where shear bands were observed may develop at the crack tip and the toughness test needs to be validated and mostly requires a fatigue pre-crack to

avoid extensive plasticity (and extensive blunting) ahead of the notch radius.

Among the various methods, indentation-based ones (IF) have been widely used in determining the fracture toughness of brittle materials. This is primarily because of the ease for the specimen preparation, and further for crack nucleation from a sharp indenter. However, the use of IF methods calls for caution, not only because of the complexity of the microcracking pattern, but also because of the significant contribution of densification and pile-up to the formation of the imprint.[37-39] The occurrence of densification already drove Arora et al.[38] to differentiate between anomalous glasses and normal ones, in view of their indentation-cracking behavior. Chiefly four-fold coordinated glasses (silica-rich glass for example) were found to experience densification and to exhibit cone cracking (anomalous behavior) beneath a Vickers indenter. The following statement was made five years ago by Lawn et al.[40] in a review paper on sharp indenter probing of materials: "Some materials... may undergo densification by compaction or phase transformation from the intense hydrostatic compressive stresses within the immediate contact zone...In such instances the volume of the indentation is more readily accommodated within the compaction zone, diminishing the intensity of any residual stresses. Expanding cavity models are then no longer valid". High pressure investigations conducted in the past fifteen years on series of glasses from different chemical systems, either by isostatic loading or by sharp contact loading, uniformly concluded to densification mostly contributing to over 40 % of the indentation deformation[39,41-48]! The indentation cracking behavior is clearly very sensitive to the extents to which densification and pile-up develop[42-48]! Interestingly, Poisson's ratio (ν) shows up as an index allowing for a simple (but rather rough) discrimination between densification and shear flow.[41–43] At low ν, densification prevails and ring/cone hertzian-like cracking is observed (a-SiO_2 and SiO_2-rich glasses, borosilicate glasses), so that radial cracks are very limited and indentation cracking methods result in K_c values being overestimated. At large ν shear (pile-up) is favored and radial as well as lateral cracking occur, unless ductility and toughness prevent from extensive cracking, as for Zr-based metallic glasses (Figure 2). The volume of the affected zone might be very different for glasses having

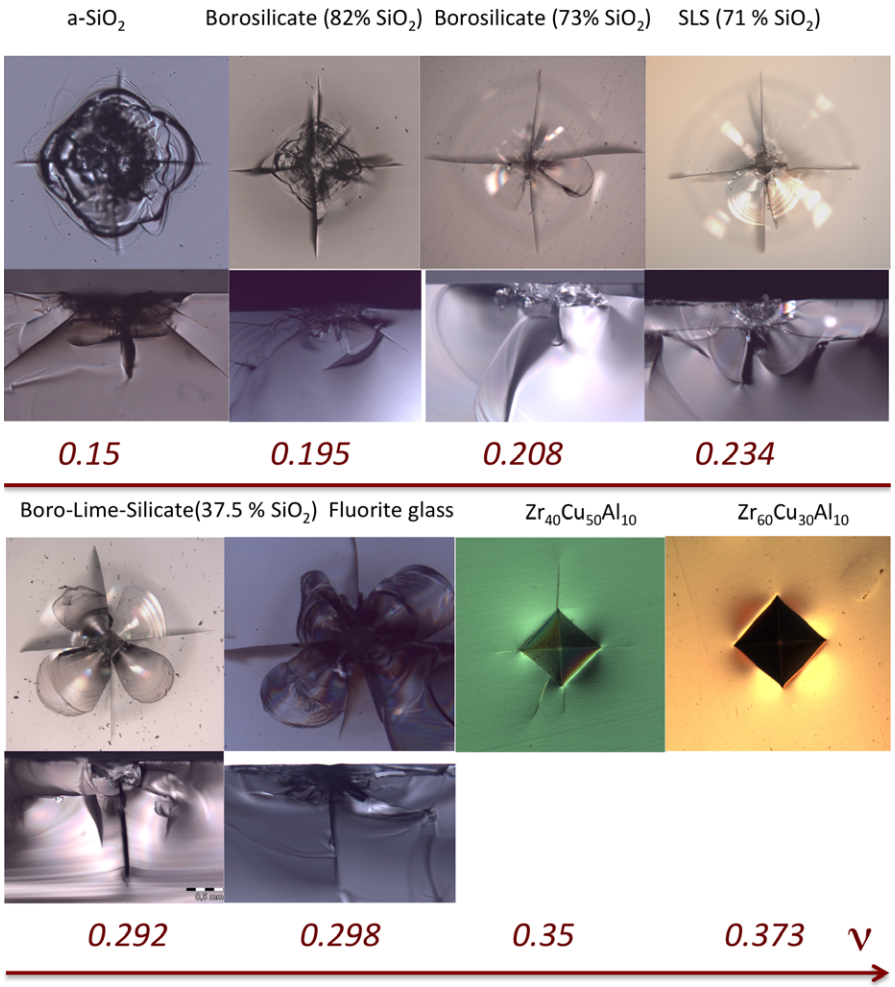

FIGURE 2 Glasses from different chemical systems indented for 15 seconds in ambient conditions using a Vickers diamond indenter. See Ref. [43] for details regarding the composition and the loading specifications

similar hardness and Young's modulus depending on their respective abilities for densification and shear flow. Therefore one can easily understand that K_c values determined by the IF test may be very different from those measured by self-consistent methods.[49] Typical examples of situations where the indentation cracking behavior would lead to greatly overestimate K_c are shown in Figure 3.[50-52] Glasses displayed in Figure 3 can be viewed as resistant to indentation cracking, but this does not necessarily entail a large toughness! An attempt to account for the elastic recovery and the pile-up of matter by Feng[53] gave agreement between experiments and FEM modelling in the case of perfect elasto-plastic materials (i.e. not for glass!). A classical plastic yield criterion sounds inappropriate in view of the physics of densification, which is a kinematically bounded process and implies strain-hardening, as well as concomitant changes of the elastic moduli. Besides, none of the equations associated with the estimation of K_c from IF method (and there are over 19 of such equations[13]) yields a value close within 5% to those obtained by standardized methods that are recognized as self-consistent, regardless of the glass composition. A comparative study of IF with other methods such as SEPB, CN and CSF yields the same conclusion considering ceramics with controlled microstructures.[54,55] The recently obtained data regarding densification and shear-flow phenomena in glasses are very encouraging and open new realms of possibilities for the search of sensible fracture toughness expressions dedicated to this class of materials.[41,43] In the case of glasses, K_c values as determined by IF are typically 20%-60% shifted from SEPB or CN values, and the shift differs from one chemical system to the other. For example Vullo et al.[49] reported values ranging between 0.37 and 0.53 MPa·$\sqrt{m}$ by IF method with different equations, while they obtained 0.62 by the CN method for the SF6 lead silicate glass from Schott (Table 2). For a lead-copper-borate glass with 10 mol% CuO (Table 2), IF values are between 0.35 and 0.8 MPa·$\sqrt{m}$ depending on the equation,[56] while the SEPB one is 0.42 MPa·$\sqrt{m}$. A relatively good correspondence is noticed though for a classical window glass (soda-lime-silica system) which was often included in the series of materials used to calibrate the method.

On the one hand, IF, CSF, and IS methods are simple evaluation methods for K_{Ic}, but remain essentially empirical and inaccurate. On the other hand, SEPB and CN methods are based on well-defined crack geometries and benefit from self-consistent expression for the stress intensity factors.

In the SEPB test,[16,17,24,25] a popped-in pre-crack is prepared on the single edge of the specimen, so that the tip radius of the popped-in crack is atomically sharp, and problems of the crack-tip roundness or notch width are solved. Some specifications regarding the bridge indentation need to be accounted for though. The SEPB method uses the bridge indentation to pop-in a sharp pre-crack from a notch slit or from an alignment of several indentations with radial cracks. The bridge indentation setup consists of two parallel and well-polished bridge anvils. An indented or notched specimen is sandwiched between the anvils and loaded in compression until a pre-crack pops in (acoustic emission can be used to monitor the event and to control the machine actuator). Other techniques to produce the sharp pre-crack were also reported in previous papers.[57-59] K_{Ic} is then calculated from the pre-crack depth, and from the load at fracture of the pre-cracked beam during a three- or four-point bending test. Although operator skill and experience are required, the crack-tip obtained in the SEPB method is ideal for determination of K_{Ic}, so that the SEPB method is hence recommended to measure a glass toughness.

The CN method[17,26–28] is an alternate suitable self-consistent technique. The chevron(triangular) notch is machined not only in the four- or three-point bend specimen but in the short bar or rod. Since the CN specimen makes it possible for a crack to propagate stably, the short bar or rod specimen is used for determination of fracture surface energy from the load vs displacement curve during stable fracture. The fracture origin of the CN specimen is always located at the tip of chevron. Fracture toughness can be calculated from the maximum load, corresponding to a critical crack extension and thus to a sharp crack tip, and from the sample geometries without measuring the crack length.

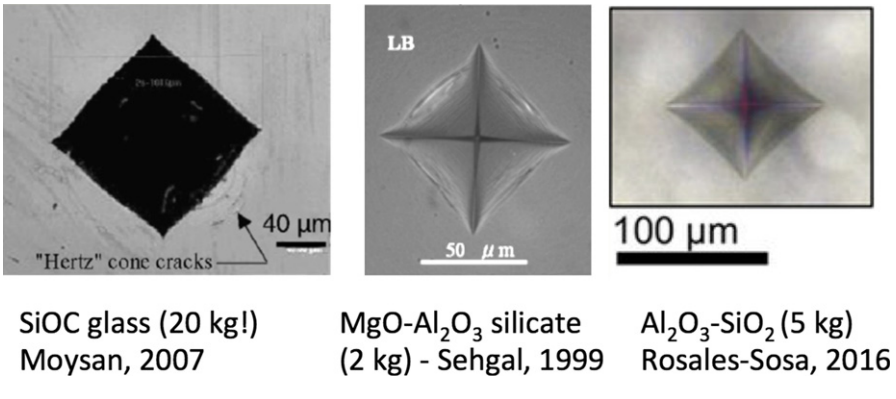

FIGURE 3 Vickers imprints left at the surface of a SiOC polymer-derived glass, a silica-rich magnesium-aluminosilicate glass (so-called low brittleness glass) and an alumino-silicate glass (bead synthesized by the levitation technique with a laser heating), from Refs. [50-52]

TABLE 2 Fracture surface energy and fracture toughness of glasses from different chemical systems. The theoretical value for K_{Ic} is derived from γ, E and ν using the plane strain assumption. Experimental errors are typically of ±1 GPa for the elastic moduli and ±0.05 MPa·√m for fracture toughness as measured by the SEPB or CN methods. Numbers in brackets give the nominal composition in mol%. Minor constituents (typically <2 mol%) are omitted in the commercial glass compositions, as extracted from the corresponding references, and might be slightly inaccurate

	Experimental					Theoretical			
Glass	ρ (g cm^{-3})	E (GPa)	ν	K_{Ic} (MPa·m$^{0.5}$)	Method	V_0 cm^{3}mol^{-1}	C_g	γ (J m^{-2}) D_0 (A-B)/Sun	K_{Ic} (MPa m$^{0.5}$) D_0 (A-B)/Sun
a-SiO_2	2.2	70	0.15	0.73	DCC (in vac)[94]	9.10	0.456	3.62/2.104	0.718/0.549
$Si_{0.25}Na_{0.92}Ca_{0.035}Mg_{0.021}O_{0.602}$ (Planilux WG Saint-Gobain) $SiO_2(71)Na_2O(13)MgO(6)CaO(10)$	2.49	72	0.224	0.68-0.72	CN-SEPB[117]	8.23	0.496	3.55/1.927	0.734/0.54
$Ti_{0.013}Si_{0.287}Na_{0.067}O_{0.633}$ $SiO_2(86)Na_2O(10)TiO_2(4)$	2.34	65.3	0.215	0.68	SEPB[44]	8.69	0.473	3.57/2.01	0.7/0.524
$Ti_{0.013}Si_{0.270}Na_{0.1}O_{0.617}$ $SiO_2(81)Na_2O(15)TiO_2(4)$	2.39	66.1	0.201	0.6	SEPB[44]	8.53	0.479	3.55/1.956	0.699/0.519
$Ti_{0.013}Si_{0.253}Na_{0.133}O_{0.6}$ $SiO_2(76)Na_2O(20)TiO_2(4)$	2.46	63.9	0.232	0.6	SEPB[44]	8.29	0.491	3.55/1.915	0.692/0.509
$Ti_{0.037}Ba_{0.111}Si_{0.222}O_{0.63}$ $SiO_2(60)BaO(30)TiO_2(10)$	3.75	74.9	0.276	0.47	SEPB[102]	8.90	0.519	0.861/0.748	0.374/0.348
$Si_{0.196}Na_{0.008}K_{0.005}Pb_{0.196}O_{0.595}$ (Schott SF6 lead silicate) $SiO_2(49.3)PbO(49.1)Na_2O(1)K_2O(0.6)$	5.18	55	0.248	0.62	CN[49]	10.8	0.425	2.83/1.378	0.576/0.402
a-B_2O_3	1.85	17.4	0.26	0.95-1.3	IF[106]-SENB[108]	7.53	0.495	4.99/3.238	0.432/0.348
$Pb_{1/7}B_{2/7}O_{4/7}$ $B_2O_3(50)PbO(50)$	5.69	57.5	0.289	0.35	SEPB[56]	7.36	0.565	0.881/0.260	0.332/0.181
$Pb_{0.114}B_{0.286}Cu_{0.029}O_{0.571}$ $B_2O_3(50)PbO(40)CuO(10)$	5.34	67.4	0.298	0.42	SEPB[56]	7.07	0.574	0.864/0.275	0.358/0.202
$Zn_{1/7}B_{2/7}O_{4/7}$ $B_2O_3(50)ZnO(50)$	3.42	80.9	0.33	0.4	SEPB[56]	6.31	0.577	0.621/0.501	0.336/0.302
$Si_{0.215}K_{0.031}B_{0.123}O_{0.631}$ (NEG) $SiO_2(70)B_2O_3(10)Al_2O_3(10)$	2.28	64	0.233	0.73	SEPB[78]	8.19	0.512	4.085/2.187	0.744/0.544
$Si_{0.226}Al_{0.065}B_{0.065}O_{0.645}$ (NEG) $SiO_2(70)B_2O_3(20)K_2O(5)$	2.48	70	0.208	0.79	SEPB[78]	7.7	0.522	4.025/2.356	0.767/0.587
$Si_{0.235}B_{0.039}Pb_{0.098}O_{0.627}$ (NEG) $SiO_2(60)Al_2O_3(25)B_2O_3(5)$	4.44	63	0.261	0.66	SEPB[78]	8.42	0.513	3.67/1.94	0.704/0.512

(Continues)

TABLE 2 (Continued)

Glass	Experimental					Theoretical			
	ρ (g cm^{-3})	E (GPa)	ν	K_{Ic} (MPa·m$^{0.5}$)	Method	V_0 cm^{3}mol^{-1}	C_g	γ (J m^{-2}) D$_0$ (A-B)/Sun	K_{Ic} (MPa m$^{0.5}$) D$_0$ (A-B)/Sun
$Si_{0.245}Na_{0.024}Al_{0.012}B_{0.079}O_{0.639}$ (Corning 7740 Pyrex) $SiO_2(81)B_2O_3(13)Al_2O_3(2)Na_2O(4)$	2.23	63.7	0.2	0.68	CN[105]	8.46	0.478	3.88/2.162	0.718/0.536
$P_{0.216}Al_{0.038}K_{0.056}Ba_{0.023}Nd_{0.008}O_{0.659}$ (Schott LG 750) $P_2O_5(58)Al_2O_3(12)K_2O(16)$ $BaO(13)Nd_2O_3(1)$	2.83	50	0.256	0.48	CN[49]	8.60	0.562	2.546/1.275	0.522/0.369
$Y_{4.70}Mg_{6.56}Si_{16.78}Al_{11.67}O_{51.5}N_{8.75}$ $SiO_2(46.7)AlN(24.4)MgO(18.3)$ $Y_2O_3(6.5)Al_2O_3(4.1)$	3.18	134	0.28	1.18	CN[115]	7.27	0.559	3.729/2.185	1.041/0.797
$Y_{0.123}Si_{0.185}Al_{0.07}O_{0.55}N_{0.075}$ $SiO_2(52.8)Y_2O_3(25.2)Al_2O_3$ $(14.3)Si_3N_4(8.4)$	4.0	150	0.29	1.05	IF[112,113]	6.96	0.608	4.039/2.296	1.15/0.867
$Sr_{0.21}Si_{0.221}O_{0.4035}N_{0.1655}$	3.9	104	0.305	0.95	IF[113]	8.56	0.547	3.24/1.75	0.862/0.634
$Ge_{0.25}Se_{0.75}$	4.36	16.1	0.281	0.222	CN[117]	17.7	/	1.77/0.98	0.25/0.18
$Ge_{0.3}Se_{0.7}$	4.32	17.9	0.264	0.210	CN[117]	17.9	/	1.55/0.78	0.24/0.17
$Zr_{55}Cu_{30}Al_{10}Ni_5$	6.83	81.4	0.38	35-53	Precrack SENB[126]	11.0	0.745	2.4-3.6	0.48-0.58

3 | WHAT WE KNOW ABOUT THE ULTIMATE GLASS STRENGTH AND THE ACTUAL WEAKNESS OF GLASS?

3.1 | The ultimate glass strength

The ultimate glass strength, or the intrinsic glass strength, can be estimated from the failure strength or strain at fracture of pristine (supposedly flaw-free) fibers in inert condition. The intrinsic failure characteristics are then derived by making some assumptions regarding the constitutive law for the non-linear elastic behavior, especially at such a high stress level. In the previous review papers, Kurkjian et al.[60,61] explain that the intrinsic strength should include effects of intrinsic features such as defects frozen-in structural inhomogeneity, but not the effects of extrinsic contact damage. Therefore, it is considered that the intrinsic glass strength is a function of temperature, fictive temperature, strain rate, and glass composition. Since the practical glass strength is in general controlled by the extrinsic flaws and/or by slow crack growth, it is very difficult to evaluate the effects of the glass composition on strength (See the Mould plot.[62] Figure 4). In the Mould plot, log σ is plotted against log a according to Equation (1). From this equation, it is found that fracture toughness of glass shifts the position of the Mould's plot up or down. As shown in Table 2, however, the compositional variation of fracture toughness is much smaller than the variation of glass strength with flaw depth. In order to evaluate the effect of composition on glass strength, one should obtain the strength of glass containing only inherent flaws. In fact, Brambilla and Payne[63] reported that silica nanowire manufactured by "modified flame brushing technique" exhibits considerably high tensile strength, ~26 GPa which is close to the theoretical limit of silica strength as estimated from Young's modulus, the mean interatomic distance, and the surface energy.

The exceptionally high strength of fibers free from extrinsic flaws requires the use of a two-point bending loading set-up. This method is advantaged by the absence of fiber gripping devices, and can easily be used in inert condition (liquid nitrogen). One disadvantage though lies in the difficulty of determination of the failure stress, since the strain is the sole experimentally available parameter. Besides, the intrinsic fracture stress is associated to unusually large strain, over 0.1. In this range, the consititutive law is no longer linear. Nevertheless, some attempts have been reported to obtain the precise values of the intrinsic failure stress from the two-point bending failure strains.[64,65]

The variation of the intrinsic strength with the composition of oxide glasses was investigated with this technique. The failure strain of binary silicate and sodium aluminosilicate glasses was found to increase with an increasing number of non-bridging oxygen atoms (NBO) in glass.[66,67] Figure 5 shows a relation between the intrinsic failure strain of binary silicate glasses and NBO concentration.[68] The authors explained that the presence of NBO appears to allow the glass network to deform more prior to fracture. In addition, it has been also reported that the intrinsic strength of binary sodium silicate glasses scales with their hardness.[61] This observation is interesting, because hardness is a measure of flow under a sharp indenter while fracture occurs under tension. Authors put forward the hypothesis that both failure in tension and flow during indentation are associated with the breakage of Si–O–Si bonds or Si–O–Na bonds in glass. Although there has been long lasting debates about a relation between hardness and strength,[69,70] the physics behind still remain to be elucidated. This is probably due to the complicated mechanism of permanent deformation in glass at ambient conditions.

The other interesting phenomenon on two-point bending strength of glass fibers is Inert Delayed Failure Effects (IDFE). IDFE means the rate dependence of the intrinsic strength in inert condition. Unlike the normal fatigue behavior of glass in humid condition, the failure strain increases with decreasing the strain rate. Figure 6 shows one example of IDFE for Na_2O–SiO_2 system.[68] The authors claim that IDFE is related to silicate network motions associated with non-bridging oxygens (for example, internal friction of NBO). Although the detail mechanism of IDFE is still unclear, such an energy dissipation process as ion motion under high tensile stress may control the ultimate glass strength. Further experimental and modelling works will be highly required in this exciting research field. Actually, recent MD studies of intrinsic nano-ductility in glass may help us understand the ultimate glass strength.[71]

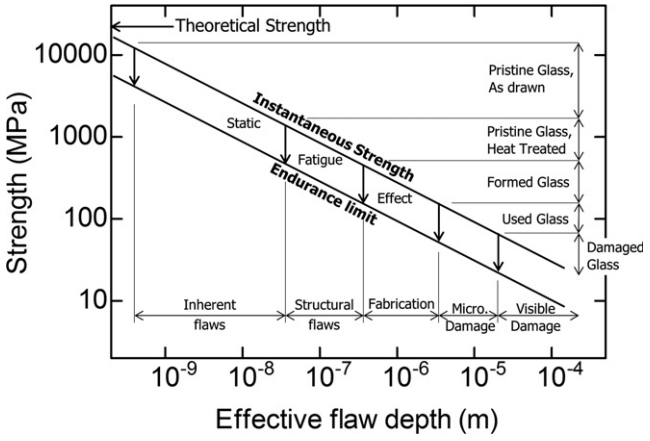

FIGURE 4 Strength vs effective flaw depth for glass[62] (The original figure is modified using SI units.)

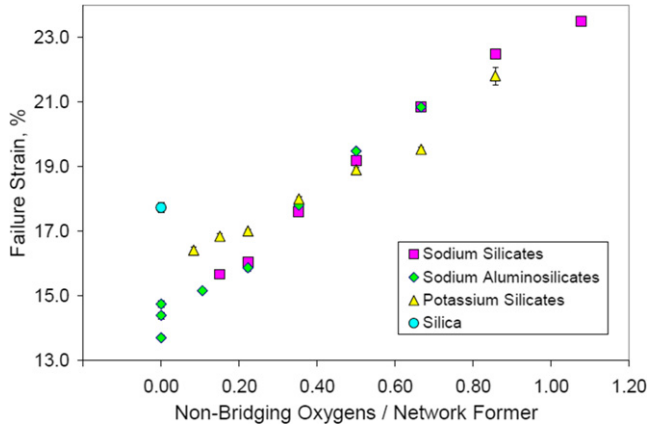

FIGURE 5 The effect of non-bridging oxygens on the failure strains of silica, binary silicate, and sodium aluminosilicate glass fibers in liquid nirogen[68]

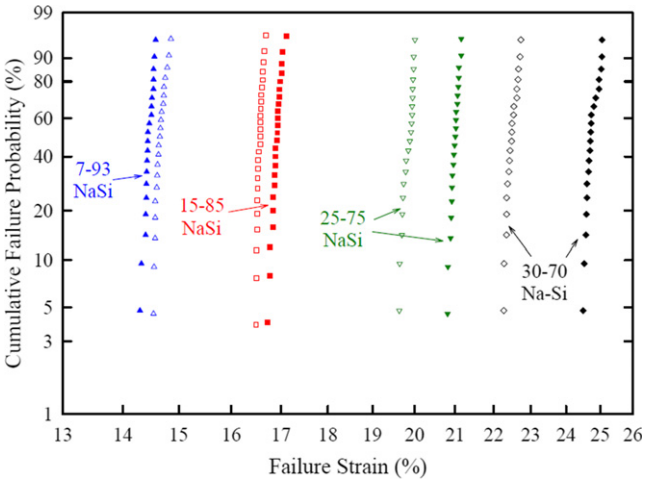

FIGURE 6 Weibull distributions of the liquid nitrogen failure strains for $x\mathrm{Na_2O}$-$(1-x)\mathrm{SiO_2}$ glasses using faceplate velocities of 4000 μm/s (open symbols) and 50 μm/s (closed symbols)[68]

3.2 | Surface flaws, indents and associated residual stresses

As stated in 3.1), the practical glass strength decreases due to the extrinsic contact damages. Even after heat treatment of a pristine glass at far below T_g, a rather striking decrease of the strength has been reported (See Figure 4). The effect of the heat treatment appears to be a surface phenomenon. The original strength is restored after subsequent etching to remove a thin layer of surface away.[72] Mould[62] described the effect of annealing as a surface phenomenon, and named the surface "flaws" that are enlarged by heat treatment as "structural flaws". However, as Mould himself recognized in his paper, the question of the size of the structural flaws remains open: Even though a size of ~10^{-7} m is predicted (Figure 4), such flaws, which should be detected, were not observed! Hydration due to water diffusion[73] is a key phenomenon to understand the strength reduction, but further experimental and modelling works will be required in this scientific area to clarify the relation between surface and mechanical properties in glass.

In principle, the size of the critical surface flaws from which fracture originates can be estimated from the actual glass strength, knowing its fracture toughness (Equation 1) (Figure 4). In order to get some insight into the stability of natural flaws, the indentation test shows up as very interesting technique. An indentation leaves a permanent imprint, which is the source for a residual stress field that chiefly arose from the volume strain around the "plastic" or "process" zone. If the stress concentrates at the tip of the natural flaw in glass, the pop-in of crack can be observed. This is called the indentation-induced cracking, and the onset for cracking can be detected by slowly increasing the indentation load and monitoring acoustic emission, or direct in-situ observation. Actually the driving force for the opening of cracks from the indentation corners depends much on the glass composition. The *E*/*H* ratio and Poisson's coefficient were identified as key parameters to estimate the intensity of the relevant stress component.[42,43] This is illustrated in the isocontour map in Figure 7 for the tangential normal stress $\sigma_{\phi\phi}(\theta = \pi/2)$ (where $\phi\phi$ is the angle around the loading axis, and θ the angle to it; $\theta = \pi/2$ corresponds to the surface). It is noteworthy in Figure 7 that glasses with large ν will develop large residual stresses and are prone to extensive radial cracking. However, bear in mind that a sufficient toughness might impede the formation of cracks, as for example the indentation edges become blunted. This is presumably why ductile metallic glasses exhibit no visible cracking, and to a lesser extent why oxynitride glasses (with $K_{Ic} > 1$ MPa·$\sqrt{m}$) experience limited cracking, while sulfophosphate and chalcogenide ones suffer from extensive damage. Remark in Figure 7 that the low brittlness glasses developed by Sehgal et al.,[51] with *E*/*H*~14.7 and ν~0.18 are precisely in the red coloured areas corresponding to the zero-stress contours for $\sigma_{rr}(\theta = \pi/2)$ (and in the compressive side for $\sigma_{rr}(\theta = 0)$ and $\sigma_{\phi\phi}(\theta = \pi/2)$).

Indentation tests with sharp indenters are of great interest to evaluate the resistance of glass to crack initiation, which can also be viewed as a criterion for the resistance toward mechanical surface damage. The critical load (P_c) from crack initiation at the indentation site is not easily measured. First of all, different types of cracks stem from an indentation loading experiment, some of them being hardly detectable either because they are located beneath the surface or because they align with the indentation edge.[74] Besides, indents that seem to be optically crack free, turn out to have some microcracks when observed at

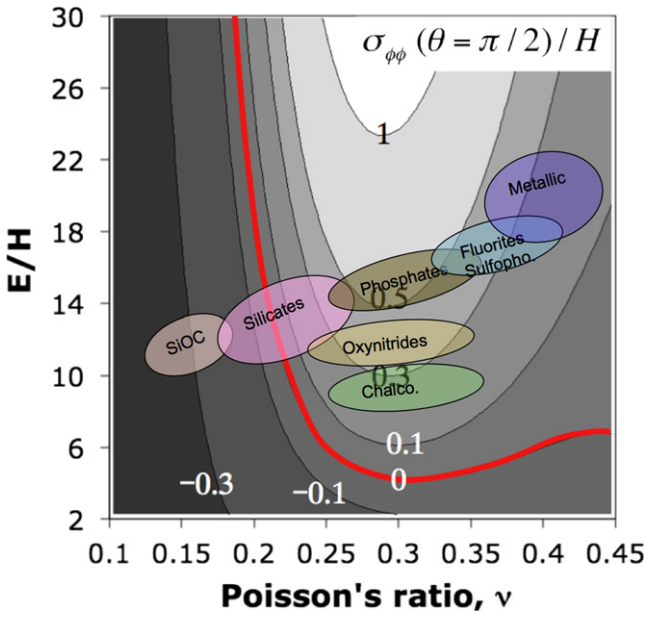

FIGURE 7 Indentation cracking map showing the intensity of the driving force (i.e. the normal tangential stress component $\sigma_{\phi\phi}$ at the surface ($\theta = \pi/2$)) for the opening of radial cracks from the indentation corners (from Ref. [43]). The red line is where $\sigma_{\phi\phi}$ vanishes. Numbers indicate the stress intensity normalized to hardness on the corresponding iso-contour

much smaller scale by AFM or SEM. In addition, some cracks show up with some delay, after complete unloading. The critical indentation load corresponding to either the occurrence of cracks from two indentation corners (Vickers test) or to achieve a 50% cracking probability[75] is illustrated in Figure 8 for several families of glasses, together with the prediction of two popular models developed by Lawn et al.[1] and Hagan.[76] Although these latter models provide a qualitative description of the observed tendencies in some cases, they don't seem appropriate for a quantitative estimation of P_c for glasses with various compositions. P_c does mostly not follow a K_{Ic}^4/H^3 relationship, as was proposed in Refs. [1,76]. To the best knowledge of the authors, no model is able to provide a reliable prediction of the micro-cracking initiation load in glasses yet. Again, models inherited from an elasto-plastic analysis of the mechanical fields at the indentation site are poorly suited to glasses. Densification and the pile-up of matter by isochoric shear, as discussed in previous papers,[42-44,78] need to be taken into account. The mean crack length over the four corner cracks produced by a 9.81 N load (Vickers test) is shown for sake of comparison for different glass systems in Figure 9. Of course, direct measurement or determination of the residual stress is of primary importance to evaluate the critical load for indentation cracking. Birefringence technique,[79] cathodoluminescence technique,[80] and modelling[81,82] are on-going works to obtain the residual stress map around the indentation imprint.

4 | DEPENDENCE ON THE GLASS ATOMIC STRUCTURE AND COMPOSITION

In order to compare the fracture surface energy and the fracture toughness of glasses from different chemical systems or with different compositions within a given system, it is interesting to reach theoretical expressions for both γ and K_{Ic} shedding lights on the particular importance of some structural characteristics such as the atomic binding energy, the atomic packing density, the specific mass, the molar volume etc. A relatively simple approach to predicting γ and K_{Ic} in a quantitative manner consists in assuming that a propagating crack extends following a path disrupting the weakest links of the energy landscape and to estimate the surface energy from the bond strength and the bond concentration along this fracture surface. Although this theoretical analysis eludes any relaxation or surface reconstruction mechanism on the fracture path, and further ignores the fine structural details of the atomic network, it was found to provide γ and K_{Ic} values in agreements with the experimental ones when such values were available.[83] In this approach, the intrinsic (or theoretical) fracture surface energy is obtained from the surface density of representative structural units and from the relevant bond strength. Let ρ and M_o be the glass density (specific mass) and the molar mass of a representative unit (gram-atom of glass), then the volume concentration of the gram-atom is expressed as:

$$\rho_v = \frac{\rho}{M_o}\mathcal{N} \tag{3}$$

where $\mathcal{N}$ is Avogadro number.

The surface concentration is then

$$\rho_s = \left(\frac{\rho}{M_o}\mathcal{N}\right)^{2/3} \tag{4}$$

A plausible value for γ is obtained by considering the number and the type of bonds involved in the fracture process as the crack proceeds through the considered structural unit. Let x_i be the stoichiometric fraction of the species involved in the ith diatomic bonding energy U_{oi} (in J mol^{-1}), between the ith cation and a first neighbor oxygen anion in the case of an oxide glass, and let n_i be the number of such bonds supposed to be broken as the crack front propagates to the next unit, then γ is expressed as

$$\gamma = \frac{1}{2}\left(\frac{\rho}{M_o}\right)^{2/3}\mathcal{N}^{-1/3}\sum_i x_i n_i U_{oi} \tag{5}$$

where the ½ prefactor on the right hand side member accounts for the fact that the bond disruption process leads

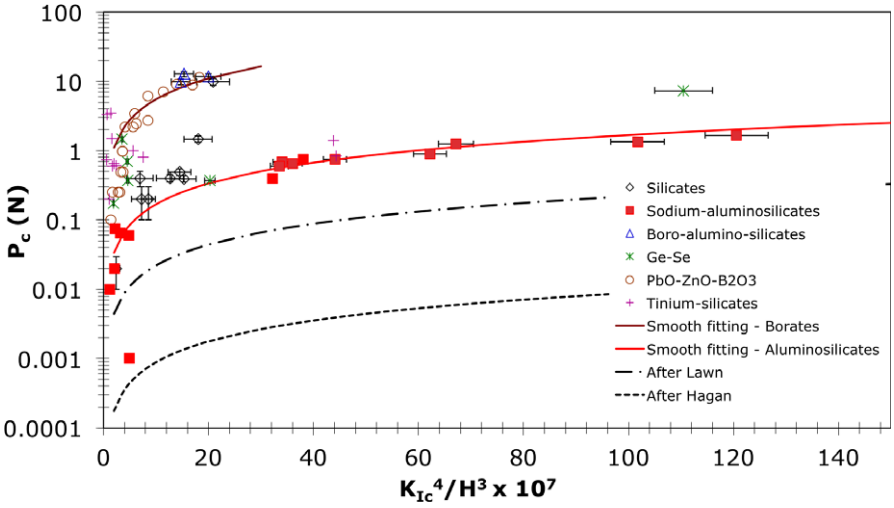

FIGURE 8 Critical load for indentation cracking (Vickers test/surface radial cracks). P_c is defined as the load required to generate two radial cracks on average or to achieve a 50% cracking probability.[75] H is hardness (Pa) and K_{Ic} is fracture toughness (Pa $m^{0.5}$). Data from Refs. [41,42,44,77,78,116]. Models by Lawn et al. and Hagan are from Refs. [1] and [76] respectively

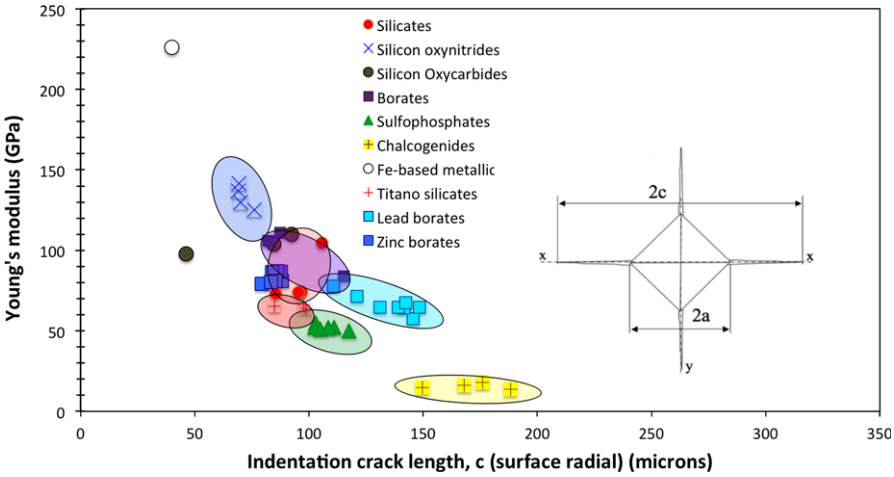

FIGURE 9 Correlation between Young's modulus and the Vickers indentation crack length (surface cracks) for a 9.81 N load

to the formation of two complementary surfaces (a crack has two walls).

The bond dissociation energy in polyatomic molecules, radicals or structural units is notoriously difficult to measure accurately since the mechanism involved in the measurement is usually not well known. In order to estimate the A–O cation-oxygen bond strength, where both elements participate in a crosslinked glass network, Sun[84] proposed to consider the dissociation enthalpy $D°(A_xO_y)$ of the A_xO_y compound and to divide this quantity by x and by the coordination number of A to oxygen. Recall that $D°(A_xO_y)$ is simply the sum of the atomization enthalpy (gaseous species) of the atoms $(x\Delta_f H(A,g) + y\Delta_f H(O,g))$ and the negative of the enthalpy of formation of A_xO_y $(\Delta_f H(A_xO_y))$. A major disadvantage of this method is that the coordination number is required, and this number might experience changes from one chemical system to another, and even within a glass network for a given element. Besides, this approach ignores any other interactions, such as the repulsive O–O one in the first coordination shell around A, which would result in an underestimation of the attractive A–O bond energy. Another way consists in simply taking the A-B bond dissociation energy in the AB diatomic molecule, D°(A-B), which is the standard enthalpy change for the fission reaction, usually measured by spectroscopy or mass spectrometry. Of course, in this latter case, the bond electronic properties is usually quite different from the actual ones in the connected network. Indeed, the fission enthalpy can be seen as an upper bound, corresponding to the limit case where all the binding energy concentrates in a unique bond. In what follows, the first way is referred to as Sun's method, and the second one as the D°(A-B)′ method. Both ways are further explored and discussed for different chemical compositions.

The actual volume occupied by the gram-atom of glass is mostly significantly larger than the sum of the volumes of the individual atoms constituting this unit, as estimated from the ionic radii (i.e. assuming a particular value for the corresponding valency and coordinence) taken from the literature,[85] $\sum_i 4/3\pi\, x_i r_i^3$. This is where the atomic packing density comes into play

$$C_g = \frac{\sum_i 4/3\pi\, x_i r_i^3}{V_o} \quad (6)$$

where V_o is the molar volume (gram-atom).

Let's further write $<U_o>$ the mean bond strength considered in the fracture process, $<U_o> = \sum_i x_i n_i U_{oi}$, then γ can be written

$$\gamma = \frac{1}{2}\left(\sum_i 4/3\pi\, x_i r_i^3\right)^{-2/3} \mathcal{N}^{-1/3} C_g{}^{2/3} <U_o> \quad (7)$$

This expression emphasizes the independent roles that play C_g and $<U_o>$. Equation (5-7) and $K_{Ic} = (2\gamma E')^{1/2}$ (E': the plane strain Young's modulus) were applied to 22 glasses with known elasticity and fracture toughness characteristics (Table 2) (Figure 10), including 7 commercial glasses from different glass making companies. The way the calculation is done is discussed case by case for the different chemical systems under scrutiny. These few examples show that an efficient packing (large C_g) might compensate a weak bonding energy and vice-versa, and that a minimum surface energy estimation is in agreement with the experimental values. A simple bond energy approach of fracture toughness was already proposed by previous authors[86] for brittle materials. In this former study the surface energy for the fracture of crystalline solids was calculated for various crystallographic orientation using the actual lattice constants and the relevant bond dissociation energies. K_{Ic} was then derived accounting for the elastic moduli for the crystallographic orientation of concern. The model was extrapolated to simple amorphous materials having the same stoichiometry as the studied crystals assuming that the actual surface energy of the glass scales with its density and is proportional to the one of the crystal, which results in overestimations for γ and K_{Ic} of most of the studied glasses.[86] In the present model, the glass density comes to the power 2/3

$$\gamma_{(glass)} = \gamma_{(crystal)}\left(\rho_{(glass)}/\rho_{(crystal)}\right)^{2/3} \quad (8)$$

Recall that an elastic moduli reflects a volume density of energy (a Pa is a $J\cdot m^{-3}$) and that some correlation exists between the bulk modulus K, the overall dissociation enthalpy ($<\Delta H_{a\ dissoc}>$) of the glass network,[87-89] and the molar volume ($V_o = M/\rho$), then neglecting Poisson's ratio effect, Young's modulus [$E = 3(1-2\nu)K$] is proportional to the glass density

$$E \propto \left(<\Delta H_{a\ dissoc}>/M\right)\rho \quad (9)$$

Finally, we obtain

$$K_{Ic(glass)}/K_{Ic(crystal)} \approx \left(\rho_{(glass)}/\rho_{(crystal)}\right)^{5/6} \quad (10)$$

Validity of Equations (8) and (10) supposes that crystal and the corresponding glass with the same stoichiometric composition have strong similarities from the energy viewpoint. In a comparative study of the indentation cracking behavior of (Na,Ca,K)-aluminosilicate glasses[90] a correlation was proposed between K_{Ic} and the fraction of non-bridging oxygen atoms, since K_{Ic} was found to be continuously increased from 0.92 to 1.22 MPa·√m as the non-bridging oxygen content was decreased from 34.36% to 13.36%. However, our results using the CN and SEPB methods, do not corroborate such a tendency. Pure a-SiO_2 is characterized by a K_{Ic} value very similar to the one of soda-lime-silicate glasses, and the IF method sounds inappropriate for a-SiO_2 and SiO_2-rich glasses since densification in those glasses (due to a significant free volume content) impedes the formation of the radial/median crack system. In these latter cases, the absence of surface radial cracks extending from the indentation corner cannot be related to a dramatic improvement of K_{Ic}, as discussed in Section 2.

4.1 | Amorphous silica

Although amorphous silica (a-SiO_2) is often considered as a model glass material, it possesses unique - and somewhat anomalous - properties that deserve for an independent paragraph. For instance a-SiO_2 is characterized by a low atomic packing density preventing from reaching high elastic moduli and toughness in spite of a relatively strong interatomic bonding. For pure a-SiO_2, the gram-atom writes $Si_{1/3}O_{2/3}$ and weights 20 g/mol. With a specific mass of 2.2 g cm^{-3}, this gives a molar volume of 9.1 cm^3 ($V_o = M_o/\rho$). A surface concentration of the gram-atom unit of 1.64 10^{19} m^{-2} is further obtained by means of Equation (4). Such a calculation for the surface density was already proposed to estimate the surface density of silicon atoms at the surface of silicon dioxide powder[91] and along a crack path of a-SiO_2 samples.[92] The fracture surface energy is then calculated using Equation (5) considering that one Si–O bond is broken per Si-$O_{4/2}$ tetrahedron [$n_i = 1$ in Equation (5)] since the crack front is likely to travel to the next unit once a Si–O–Si bridge between two tetrahedra is broken. The one disrupted Si–O bond per tetrahedron hypothesis was previously found to provide a maximum bound for the number of dangling bonds per unit area of fracture surface in amorphous silica.[92] Considering first the D°(A-B) estimation, a value of 799 kJ mol^{-1} is reported for the Si–O bond,[93] which gives a value of 3.62 J m^{-2} for γ. A theoretical prediction for K_{Ic} is then achieved, taking (E, ν) = (70 GPa, 0.15). A value of 0.718 MPa·√m is finally reached, which is in agreement with the experimental values (0.73) as measured using the DCC method, in inert environment to prevent against moisture effects.[94] Then, using the thermochemistry data from Ref. [93], a dissociation enthalpy of 1859 kJ mol^{-1} is

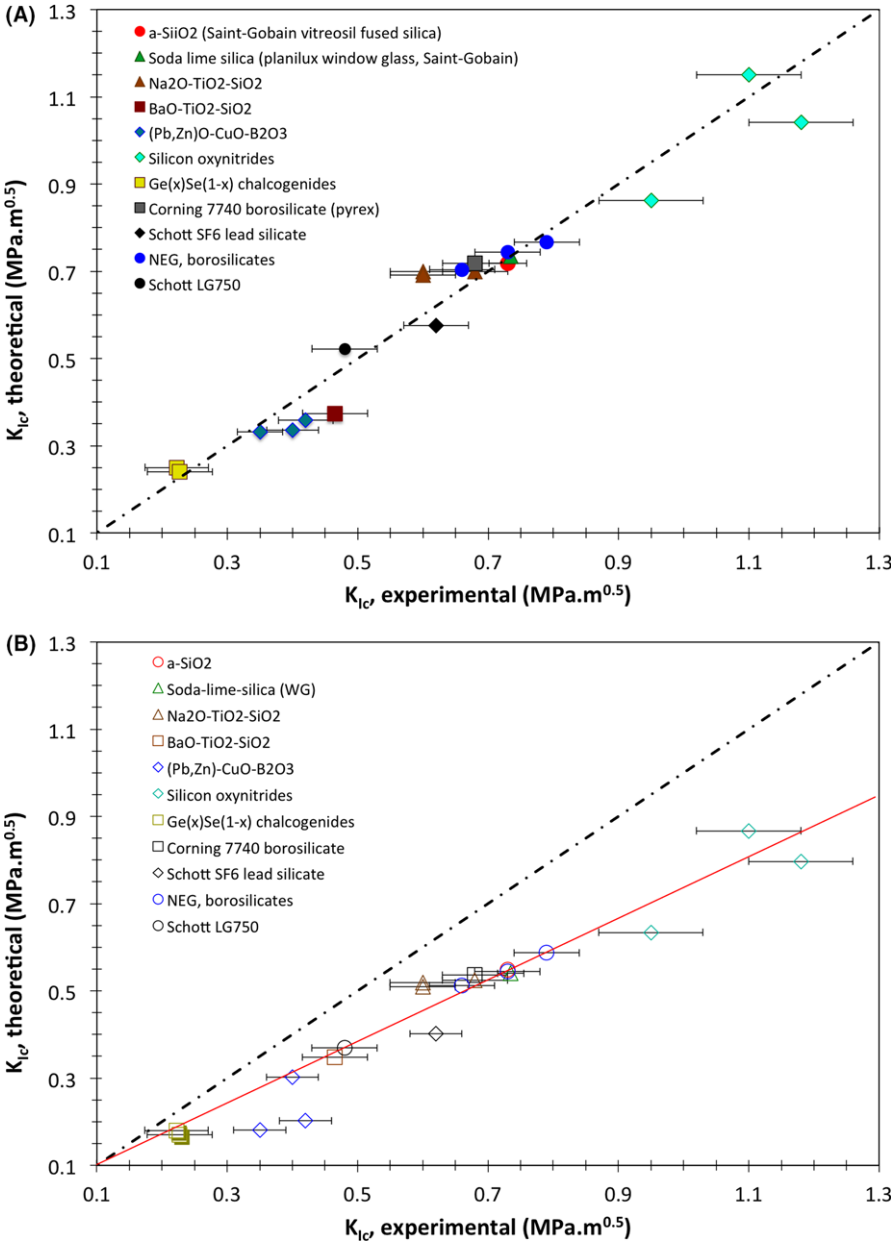

FIGURE 10 Theoretical K_{Ic} values (from γ, Equation (5)) as a function of experimental values, mostly obtained by means of self-consistent methods, when γ is calculated from (A) the bond dissociation energy of the relevant diatomic molecules (fission enthalpy), D°(A-B), or (B) the dissociation enthalpy of the constituents, D°(A_xB_y) (Sun's model)

calculated for SiO_2. Following Sun's model, this further results in a Si–O bond energy of 465 kJ mol^{-1}, and in γ and K_{Ic} of 2.1 J m^{-2} and 0.55 MPa·$\sqrt{m}$, which are significantly smaller than the experimental values. It was suggested by West et al.[95] using a semi-empirical molecular orbital calculation that fracture in a-SiO_2 is accompanied by a reconstruction of the fracture surface, according to which large (four- to six-fold) silica rings contract to form smaller rings, with consequently an energy barrier for fracture as small as 38 kJ mol^{-1} (which would lead to theoretical γ values of less than 1 J m^{-2} and K_{Ic} smaller than 0.4 MPa $\sqrt{m}$) for an Si–O–Si bridge within a sixfold ring structure. Fracture was thus expected to proceed through the large-membered rings. This reconstruction mechanism was later corroborated by the fact that the number of silanol groups counted on a fracture surface is less than the theoretical number of broken bonds.[92] Nevertheless, the agreement between the theoretical values we have reached in the present study without accounting for any reconstruction process and possible relaxation mechanism at the crack tip, and the experimental ones which were abundantly reported in the past 50 years, and always gave K_{Ic} between 0.7 and 0.9 MPa·$\sqrt{m}$ and γ between 3.7 and 4.5 J m^{-2},[94,96-100] suggests that the fracture surface energy is strongly correlated to the standard enthalpy change of the Si–O bond dissociation reaction, and to the surface concentration of such bonds. This result gives credit to the analysis of Schultz et al.[101] who concluded that fracture is a dynamic process and might therefore not comply with the structural features identified by molecular orbital

simulation or post-mortem physio-chemical investigations. They pointed out for instance that charge balance is a necessary condition for cleavage planes in ionic crystals (planes resulting in more positive charge on one side and more negative ones on the other are excluded) and that cleavage planes in crystals were often not following easy slip planes, and couldn't be easily predicted from the characteristics of the crystal structure.

In what follows, for sake of simplicity, and because theoretical results were found to compare well with the experimental ones, we will consider that the crack extends along a lowest energy path within the characteristic energy landscape of the glass atomic network.

4.2 | SiO_2-based alkaline and alkaline-earth glasses

As far as the amount of alkaline and alkaline-earth cations is small enough to keep the number of non-bridging oxygen per $SiO_{4/2}$ tetrahedron smaller than one in average the calculation is made the same way as for a-SiO_2, considering the atomic fraction (x_i) of every cation entering the stoichiometric formula of the glass, i.e. accounting for the weak A–O and/or AE–O bonds in the network. For instance, starting first with the D°(A-B) values as for a-SiO_2, $U_{oNa\text{-}O}$ = 256.1 kJ mol^{-1} and $U_{oCa\text{-}O}$ = 383.3 kJ mol^{-1}, so that the addition of Na_2O and CaO leads to a decrease of the mean gram-atom bonding energy $<U_o>$ for a soda-lime silica glass (such as a window glass, WG) in comparison to a-SiO_2. However, thanks to a significant concomitant increase of C_g, a fracture toughness value of 0.734 MPa·$\sqrt{m}$ is predicted, i.e. very close to the value for a-SiO_2, and again in agreement with the experimental value (0.68-0.72), as obtained by means of self-consistent methods in inert environment or at a velocity large enough to reduce stress corrosion.[94] It is noteworthy that the compensation of the smaller energy content by a better packing density is also effective on the elastic moduli ($E_{WG} \approx E_{a\text{-}SiO2}$). Values around 0.69 MPa·$\sqrt{m}$ were calculated for titanium sodium silicate glasses. These values are also close to the experimental ones (0.60 to 0.68)[44] but K_{Ic} tends to be overestimated as the Na_2O/SiO_2 ratio is increased from 0.116 to 0.263 (Figure 10A). It is suggested that as soon as the overall alkaline and alkaline-earth content exceeds half the silica content, at least one non-bridging oxygen forms per silica tetrahedron so that fracture is supposed to follow these weak bond path. The fracture energy and fracture toughness of a barium titanium silicate with 30 mol% BaO for 60 mol% SiO_2 were calculated accounting solely of the fractions of barium cations for $<U_o>$ in Equation (7), and values of 2.32 J·m^{-2} and 0.614 MPa·$\sqrt{m}$ were obtained. A K_{Ic} value of 0.47 MPa·$\sqrt{m}$ was measured by the SEPB method.[102] Such a difference is likely to stem from the fine details of the atomic network organization, among which barium being preferentially localized near titanium-based structural units, where Ti is mostly 5-fold coordinated to oxygen, and Ti–O bond strength being less than the Ba–O one.[103,104] Again, when the theoretical prediction is carried out with Sun's model, K_{Ic} values are typically 30% smaller than the experimental ones (Figure 10B).

It is noteworthy that theoretical and experimental values are in agreement in the case of more complicated compositions such as those of the seven commercial glasses[49,105] included in the analysis. In the case of the phosphate-based laser glass, the calculation was also done assuming one bond breakage per phosphor-based structural unit (mostly 3 single bond oxygen links and one double bond with a fourth oxygen) (Figure 10).

4.3 | B_2O_3-based glasses

Amorphous boron oxide (a-B_2O_3) and B_2O_3-rich glasses are prone to shear flow under a sharp indenter and to densification, to a lesser extent than a-SiO_2 though. This is likely why the theoretical K_{Ic} values calculated for pure B_2O_3 glass (0.35-0.43 MPa·$\sqrt{m}$, where boron is three-fold coordinated to oxygen in Sun's model) sound quite small in comparison to the results from the IF method (0.954 MPa·$\sqrt{m}$),[106,107] or from the SENB method (1.3 MPa·$\sqrt{m}$),[108] which are the only available data for a-B_2O_3 to the best of the knowledge of the authors. It is noteworthy that for the SENB method, Vernaz et al. used a 0.35 mm thick diamond disc. Such a large notch is also a likely source for the overestimation of K_{Ic}. Therefore, in the absence of reliable toughness values for a-B_2O_3, the available IF and SENB values were not plotted in Figure 10.

A series of lead and zinc borate glasses with different amount of copper were recently characterized by means of the SEPB method[14] and it turns out that for all compositions but the zinc-copper borate with 10 mol% CuO, the theoretical K_{Ic} values calculated with the D°(A-B) values under the assumption that only Pb-and Zn–O bonds are met on the fracture path, are in the 0.33-0.36 MPa·$\sqrt{m}$ interval, i.e. near the value predicted for pure a-B_2O_3. The theoretical values are in agreement with the experimental ones, which range between 0.35-0.42 MPa·$\sqrt{m}$ (Table 2), or on similar glasses by the controlled surface microflaw technique.[109] Shinkai et al.[109] found a toughness of 0.39 MPa·$\sqrt{m}$ for the B_2O_3(50 mol%)-PbO(50 mol%) composition. It is noteworthy that despite a relatively large fracture surface energy for a-B_2O_3 (γ = 4.99 J·m^{-2}), mainly due to the strength of the B–O bond ($U_{oB\text{-}O}$ = 809 and 394 kJ mol^{-1} with the D°(A-B) and the Sun's models respectively) the theoretical fracture toughness is about the

same as for the lead- and zinc- borates glasses containing 50 mol% PbO and ZnO respectively, and characterized by much smaller values for γ (<1 J m^{-2}), thanks to a much larger elastic moduli, for the Pb- and especially for the Zn-borate glasses than for pure B_2O_3 glass. Toughness values obtained by indentation cracking method on pure a-B_2O_3 are about 0.9 MPa.$\sqrt{m}$.[106,107] This is much larger than the theoretical prediction. Let's recall that borate-rich glasses (say containing more than 20 mol% B_2O_3) experience significant densification at the Vickers indentation site,[45,110] and besides that some inelastic shear flow is also likely to occur in a-B_2O_3 due to the low glass transition temperature of this glass (268°C)[111] and to the network being built on trigonal boron units. Therefore, the higher experimental values of K_{Ic} are probably related to the remarkable plasticity at the crack-tip in B_2O_3-rich glass and/or to less residual stress due to significant densification.

4.4 | Silicon oxynitride glasses

Silicon oxynitride glasses are obtained by conventional melting in argon or nitrogen atmosphere, typically up to 1750°C, adding some nitride compounds such as AlN and Si_3N_4 in the powder mixture. Nitrogen is found in the glass network to substitute for oxygen and to form Si-$(O,N)_4$ tetrahedral units, where nitrogen is mostly connected to three tetrahedra. Since nitrogen is three-fold coordinated whereas oxygen is two-fold coordinated, a signifiacnt improvement of the cross-linking degree is achieved, which results in better mechanical properties in general. For example Young's modulus as high as 150 GPa is typically measured on glasses from the RE-SiAlON system (RE: Y, Nd, Lu etc.).[112] In such glasses, the mean energy ($<U_o>$ in Equation (7)) is calculated considering that one Si-N bond is broken per Si atom involved in Si–N bonds $(Si(O,N)_{4/2}$ tetrahedra). The amount of such Si atoms is taken as $3/4x_N$ (as in Si_3N_4), and the remaining silicon forming Si–O bonds equal to x_{Si}-$3/4x_N$. For example, for the $Y_{0.123}Si_{0.185}Al_{0.07}O_{0.547}N_{0.075}$ glass composition, using the D°(A-B) approximation, $U_{oSi\text{-}N}$, $U_{oAl\text{-}O}$, $U_{oY\text{-}O}$ are equal to 437.1, 501.9 and 698.1 kJ mol^{-1} respectively. A fracture energy of 4.04 J m^{-2} and a theoretical toughness of 1.15 MPa.$\sqrt{m}$ are then easily calculated. The theoretical K_{Ic} value is quite close to the experimental one of 1.05 MPa.$\sqrt{m}$ measured by the Indentation Fracture method.[113] The theoretical values for silicon oxynitride glasses are in the range 0.862-1.15 MPa.$\sqrt{m}$ and are close to the experimental values, ranging between 0.95 and 1.18 MPa.$\sqrt{m}$,[114] including a CN measurement for one grade.[115] It is thus concluded that the toughness of silicon oxynitride glasses with 5 to 20 at.% nitrogen is near 1 MPa.$\sqrt{m}$.

4.5 | Chalcogenide glasses

The so-called "Chalcogenide" glasses are based on a chalcogen element (but oxygen) such as S, Se, Te, to which four fold coordinated elements such as Ge, Si are usually added, as well as pnictogen elements (As, Sb,...) (15th column of the periodic table). Although these glasses have the reputation of being extremely brittle, there are very few reports on the fracture properties in general and on fracture toughness in particular. The $Ge_xSe_{(1-x)}$ examples considered here were chosen because K_{Ic} as well as γ were measured by means of the CN method.[116,117] In this chemical system, Ge and Se are four fold and two fold coordinated respectively and the numbers of Ge–Se and Se–Se bonds are $4x$ and $(1-x)-2x$ respectively, provided $1-x \geq 2x$, i.e. $x \leq 1/3$, which is the case for the two compositions reported in Table 2 and Figure 10. A quite satisfactory prediction was then obtained by means of Equation (5) using D°(Ge–Se) and D°(Se–Se) equal to 484.7 and 330.5 kJ mol^{-1} respectively.[93] Dissociation enthalpies provides another mean of estimation of the bonding energies. The dissociation enthalpies of amorphous Se and $GeSe_2$ were taken from the calorimetric study by Boone et al.[118] Following Sun's approach, bonding energies of 222 and 227.6 kJ mol^{-1} were calculated for the Se–Se and Ge–Se bonds respectively, which are in agreement with those published earlier by Shkol'nikov.[119] The theoretical calculation is then performed picturing a $Ge_xSe_{(1-x)}$ glass as a mixture of $x$$GeSe_2$ and $(1-3x)$Se amorphous phases, further assuming that only one Ge–Se bond is broken per $GeSe_{4/2}$ tetrahedron, similar to the way the theoretical estimation was carried out for silicate glasses regarding $SiO_{4/2}$ tetrahedra. The theoretical prediction is then within 15% of the experimental data (Table 2). In addition, the decrease of K_{Ic} with the increase of the germanium content is also predicted. Indeed, a maximum of K_{Ic} was observed for the $Ge_{0.2}Se_{0.8}$ composition by means of the indentation fracture method.[116] This maximum isn't predicted using the present simple energy approach. Recall that K_{Ic} as estimated from the fracture surface energy is related to the crack propagation regime, and thus does not account for the physics of the initiation process. The $x = 0.2$ composition corresponds to the percolation threshold at which a change from a flexible atomic network to a rigid one is supposed to occur in the ideal case where atoms are homogeneously distributed (no chemical segregation such as phase separation etc.). Although changes are continuous with no visible transition at $x = 0.2$ when bulk properties (elastic moduli, hardness, glass transition temperature) are investigated,[120] on the contrary some transition might be seen when local or confined processes are under scrutiny. A maximum of K_{Ic} was recently observed by molecular dynamic simulation[121] and was

attributed to some blunting process at the crack tip upon loading at x around 0.2, whereas the crack is sharp as soon as it extends at $x < 0.2$ (flexible range) and in the stress-rigid range ($x > 0.2$). The situation is even more critical in the case of ductile glasses, for which the apparent values for γ and K_{Ic} greatly overestimate the intrinsic values.

4.6 | Metallic glasses

In the case of metallic glasses, the apparent fracture surface energy is much larger than the one obtained from a simple energy calculation based on a bond breaking process. In such materials where some plasticity was evidenced at the crack tip, with a "plastic" zone size extending from 10 nm for Fe- and Mg- based alloys to 10 μm for Pd-, Ti-, Cu-based alloys,[122] K_{Ic} can reach values as high as several tens of MPa·√m.[123] Values between 35 and 110 MPa·√m were reported for Zr- and Cu-based glasses,[124-126] and eventually above 100 MPa·√m for precious metal based alloys.[31] Nevertheless, in the case of non-transition metal host elements such as Ce, Ca, and Mg that develop more directional bonding through better localized f (for Ce) and sp (Ca, Mg) electrons, are much more brittle. For Ce-based and Mg-based[122,127] metallic glasses, K_{Ic} is typically smaller than 10 and 2 MPa·√m respectively. As was pointed out in an overview of the fracture toughness of bulk metallic glasses,[128] the measurement of K_{Ic} of metallic glasses raises serious problems, which partly explain why for a nominal glass composition K_{Ic} values are so much scattered. A major difficulty lies in the specimen machining, with a pre-crack or flaw sharp enough to reach the intrinsic material property. Relatively tough glasses (such as Zr- or Cu-based ones) might be suitable to operate a fatigue pre-crack, but others are too brittle. In these latter cases notched samples where mostly used, and owing to the size of the process zone (typically less than few tens of microns), the resulting so-called "notched" toughness values are likely to be much larger than the intrinsic toughness. In addition, it was reported that as the free volume content decreases (after annealing) a significant decrease in toughness follows. This observation does not seem consistent with the fundamentals of the intrinsic toughness associated to the crack propagation regime, which scales with the surface density of energy on crossing the atomic network. It could possibly be interpreted on the basis of the crack initiation process though. As was further noticed by Xu et al.,[128] the underlying physics, including the relevant length scale, still need to be elucidated. For all these difficulties inherent to metallic glasses, data plotted in Figures 1 and 9 are limited to fragile metallic glasses such as Fe- or Mg-based ones. For example, for the $Zr_{55}Cu_{30}Al_{10}Ni_5$ glass, taking the metallic radius for the metallic elements and considering that the relevant bonding energy is between the one of Cu–Cu (U_o = 201 kJ mol^{-1}) and the one of Zr–Zr (U_o = 298 kJ mol^{-1}), a values of ~0.53 MPa·√m was estimated for K_{Ic}, which is about two orders of magnitude smaller than the experimental value.[126]

4.7 | Chemical heterogeneities and phase separation

It is well known that borate-based glasses tend to be phase separated, and that in chalcogenide glasses some edge-sharing tetrahedral units might form even when the amount of chalcogen atoms isn't favorable, because these latter atoms prefer to form chains (of sulphur, selenium etc.) than inter-tetrahedral bridges introducing more constraint. There are also various properties and structural results in most glasses which suggest chemical segregation and heterogeneities, among which the mixed alkali effect for example, or the sudden drop of the viscosity as very small amounts of impurities are added to amorphous silica. Authors are aware of these complexities, which definitely affect the fracture toughness.[106,107,121,129,130] The aim of this section was to provide some straightforward and almost ab-initio picture (the glass density and the elastic moduli were taken into account) of the fracture toughness in the absence of any reliable better tool, and solely considering the nominal glass composition for sake of simplicity.

It is noteworthy that the experimental K_{Ic} values and the theoretical ones derived from Equations (2) and (5) are in agreement when the interatomic bonding energy of a given bond within the glass network is taken as the dissociation enthalpy of the diatomic molecule, further assuming that as the crack front meets a structural unit such as a tetrahedron, only one arm is broken (Figure 10A). K_{Ic} values predicted using the Sun's approach, are typically about 30% smaller (Figure 10B). Nevertheless, in both cases a quite good correspondence is noticed between experimental and theoretical values. When Sun's values for the bond strengths are used, the 1/2 prefactor in Equation (5) should be replaced by 0.71.

5 | TOWARD TOUGHER GLASSES

5.1 | State of the art

There has been long lasting efforts to improve the fracture toughness of glass. The different strategies that were identified so far as well as the remaining open questions are reviewed.[131] Extrinsic methods such as thermal and chemical tempering, and coating techniques proved quite satisfactory and lead to innovative technologies and industrial products. On the contrary, intrinsic toughening methods based on the atomic bonding character and the atomic structure still don't meet the expectations, but perhaps for

bulk metallic glasses. For given oxide compositions, within binary to quaternary chemical systems, K_{Ic} isn't found to change by more than say 20%-30% at maximum, which in absolute values means that K_{Ic} is mostly below 1 MPa·$\sqrt{m}$ and the glass behaves brittle. Some relative success was achieved by glass to ceramic conversion, by means of more and more refined thermal treatments, to meet specific glass-ceramic microstructures. In view of the abundant literature addressing extrinsic methods and glass-ceramic materials, the present analysis is limited to the role of the composition and atomic structure.

As far as the mechanical behavior at a crack tip remains purely elastic, the crack will be almost atomically sharp and, whatever the local bond strength, fracture will occur under a relatively weak far field loading. The agreement we observed between the experimental K_{Ic} data (self-consistent methods) and the theoretical prediction based on the estimation of γ, suggest that in most inorganic glasses but the metallic ones, the "propagating crack" toughness, i.e. the quantity determined from γ by means of Equation (2), is the experimentally measured characteristic, i.e. the quantity mostly estimated from the critical stress at the onset of crack extension. This leave little room for crack tip dissipation or relaxation processes. With this in mind, and consistently with the Irwin-Griffith similarity relationship (Equation (2)), K_{Ic} can be enhanced by increasing E and γ. Actually these two latter material characteristics are both intimately governed by the atomic binding energy and the packing density (Equations (7) and (9)). E can be increased by 30% relatively easily by playing on the composition within a chemical system.[88,89] For example, the addition of 10 mol% MgO and 10 mol% CaO to SiO_2 (diopside stoichiometry) leads to an increase of E from 70 to 100 GPa. This increases is expected to provide a 20% increase of K_{Ic} (say from 0.73 to 0.87 MPa·$\sqrt{m}$) regardless of the effect of γ. Much larger values for the elastic moduli were achieved by introducing significant amounts of rare-earth oxides in the composition, and/or by synthesis under controlled atmosphere (to produce nitrides or carbides), with some detrimental consequences on the transparency and on the production cost though. Unfortnately, reliable fracture toughness data on these "exotic" glasses, which are mostly not available as large batches, are lacking yet to validate this approach based on Equations (7) and (9).

In order to reduce the lever arm that expresses the concept of stress intensity factor, some energy dissipation is needed in the crack front region. Two dissipation mechanisms were identified in glasses at room temperature: densification, and isochoric shear flow. Densification occurs in glasses with large free volume contents ($C_g < 0.51$), such as silica-rich glasses. This process is favorable to the formation of Hertzian-type cracks to the detriment of radial and lateral cracks at indentation sites. Therefore densification seemingly provides a better resistance to visual damage at the surface of glasses indented with sharp objects. Efforts in this area resulted in glasses with outstanding indentation cracking resistance (Figure 3). Nevertheless, the singular stress field at the vicinity of a crack tip is associated to a positive hydrostatic component, and the maximum tensile stress is the driving force for crack extension. Therefore, the resistance to indentation cracking isn't expected to be a criterion for a better toughness. As a matter of fact, a low C_g doesn't result in a large K_{Ic}. Instead, according to Equation (7) a small C_g is undesirable, following the example of ceramic foams or porous refractories, which are known to behave brittle as the crack finds easy paths. Isochoric shear flow is observed in seemingly brittle materials when the stresses are large enough to compensate for the lack of thermal activation. Shear lines or bands are clearly seen in metallic glasses where C_g is typically larger than 0.6,[125,126,132] but ductility is particularly significant in metallic glasses with $\nu > 0.33$ such as the precious metal-based or Zr-based ones. Although shear localization observations are somewhat less convincing in non-metallic glasses, there is no question regarding a shear transport of matter, as evidenced by the formation of pile-up at indentation sites.[39,42,76,133] Shear deformation mechanisms might be activated along the crack front and was seen so far to be the major possible source for ductility. Interestingly, and in contrast with silicate glasses, there is no straightforward correlation between C_g and ν for metallic glasses. For instance, Fe-, Ti-, and Pd-based MGs have roughly the same C_g (~0.63-0.65) but their ν values spread from 0.28 to 0.43 (Figure 11).

5.2 | What Poisson's ratio tells?

Poisson's ratio can be viewed as an index of the ability of a glass to experience shear flow and shear relaxation processes at indentation site and at crack tip as well. It was reported for both oxide and metallic glasses that as ν is increased, shear flow becomes more and more important and, eventually ductility shows up. This is a direct consequence of the fact that as ν is increased, isochoric shear becomes more and more predominant over volume change. This is of course a classical result or description of the theory of linear elasticity. So what is actually obvious in the framework of elasticity, can somewhat be transposed to the irreversible flow regime. Bear in mind that any viscous or plastic flow is associated to an energy barrier that is by an overwhelming part of elastic origin. As far as shear processes are concerned, the shear modulus, μ, comes into play. Recall that $\nu = (3K-2\mu)/(6K + 2\mu)$, then

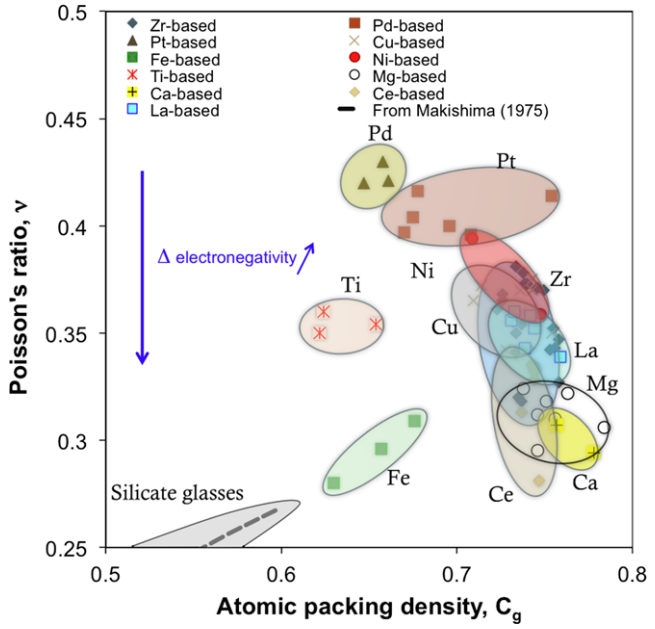

FIGURE 11 Poisson's ratio as a function of the atomic packing density for silicate and metallic glasses[135]

$$\frac{\partial \nu}{\partial \mu} = -\frac{18K}{(6K + 2\mu)^2} \tag{11}$$

Equation (11) indicates that as ν becomes larger, shear becomes easier (μ decreases). As a matter of fact, it was reported that piling-up at indentation sites becomes more and more pronounced as ν is increased.[41,42] For instance, isochoric shear transport of matter to form pile-up at the surrounding of Vickers imprints was found to account for over 40 % of the indentation volume for oxide glasses with ν > 0.28 (for example fluorite and borosilicate glasses with over ten oxide constituents) which mostly exhibit an atomic packing density larger than 0.55. Nevertheless iono-covalent glasses with large Poisson's ratio offer little room for densification, and hence experience extensive radial and subsurface lateral (leading to chips) cracking from Vickers indents (Figure 7). For example silicon oxynitride glasses with ν typically as large as 0.3 and in spite of an exceptional mechanical performance (*E* as large as 150 GPa are common for rare-earth containing silicon oxynitride glasses) are very sensitive to radial-median cracking. In the opposite, very high levels of densification (up to 80%), which correspond to Poisson's ratio below say 0.2 (as for a-SiO_2), lead mostly to the formation of ring-cone crcaks at moderate loads, and are often associated to glasses that are not easy to process (high melting points, high viscosity). In order to reduce the intensity of the stress field that builds up on indentation, it is inferred from the physics of the permanent deformation processes[41,43] that Poisson's ratio in the 0.25-0.33 range should be avoided, unless the *E*/*H* ratio is smaller than say 7 (Figure 7). Interestingly there are compositions in silica-rich alkali-alkaline earth silicate and in boro-silicate glasses for which the stress field is expected to remain very small. It turns out that the so-called "less brittle" glass developed in the 1990's by Sehgal et al.,[51] with *E*/*H*~14.7 and ν~0.18 is precisely in the optimized region (diffuse red solid line in Figure 7) with regard to the internal stress field acting as a driving force for indentation cracking. But, unfortunately, this does not entail a large fracture toughness. There are glasses with ν larger than 0.33, for instance in metallic systems,[123] but also possibly in oxynitride ones. In such materials shear plasticity is promoted and favours a ductile behavior. The fracture energy of bulk metallic glasses with ν > 0.32 exceeds the one of oxide glasses by 2 to 4 orders of magnitude.[134] Although a regain of toughness is thus expected at large ν, and is indeed observed for metallic glasses, there is no one to one relationship between K_{Ic} and ν for ionocovalent glasses (Figure 1).

5.3 | Toughness and electrons

The ease for shear deformation (flow) or for densification (pressure) is closely controlled by the nature of the prevailing interatomic bonding, and thus by the electronic band structure. Unlike oxide silicate glasses metallic glasses exhibit no straightforward correlation between C_g and ν (Figure 11). As was shown recently,[135] ν is found to increase as the difference in electronegativity between the host metal and the major solute elements decreases, so that a ductile behavior is expected for $\Delta e^- < 0.5$ (corresponding to ν > 0.33). This correlation also holds for monoconstituent oxide glasses and hence provides an explanation to the variation of ν observed for seemingly "isostructural" glasses (Figure 12). A general trend among materials and structures which proved to be scale-independent is that ν decreases as the connectivity increases.[136] This rules holds for macrostructures such as construction frames or cellular systems, as well as for atomic-scale structures, such as glass atomic networks. In ionocovalent solids, 2D and 3D atomic networks are favored thanks to the strength and the directionality of the bonding. It is thus inferred that in the case of metallic glasses, non transition metal host elements such as Ce, Ca, and Mg, develop more directional bonding through better localized f (for Ce) and sp (Ca,Mg) electrons giving rise to a relatively small ν. Some evidence for this is provided by the electronegativity difference between the host and the two major secondary elements, and the remarkable correlation found between ν and Δe^- which suggests that ν primarily depends on the bond directionality and connectivity rather than on C_g.

In the case of metals, the delocalization of the electrons and the weakness of the bond directionality is the

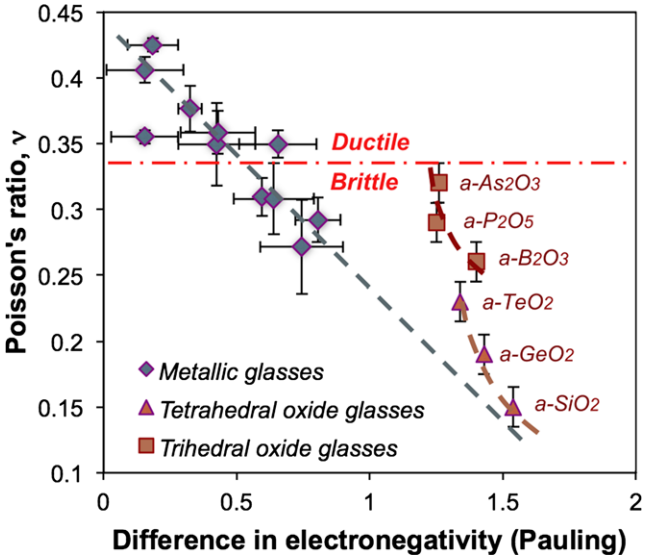

FIGURE 12 Poisson's ratio as a function of the electronegativity mismatch between the host metal and the major secondary solute elements (horizontal error bars show the interval with the two major solutes) (from Ref. [135])

fundamental source for ductility, i.e. the ease for shear plasticity and relaxation processes at crack tip as well as at the vicinity of geometrical singularities. The "good" metals are also the ductile ones! In the case of glasses, enhancing the electron mobility can be achieved by playing on the composition, introducing cations showing up with different valencies, such as Mn, Cr, Cu etc. Large amounts of copper (up to 40 mol% CuO) were introduced in phosphate[137] and in borate[14] glasses as well with the aim to favor electron hopping, and the dependence of K_{Ic} on the copper content and valency was studied. An increase of the indentation cracking resistance with the amount of Cu^{+} was noticed in the case of the phosphate glasses. However, K_{Ic} measurements (by IF method though) suggest a decrease from 0.92 to 0.56 MPa.$\sqrt{m}$ as the overall amount of copper is increased from 45 to 55 mol%. Yao et al.[14] (Table 2) have shown that by replacing lead with copper in lead borate glasses, E and C_g are increased, and both the indentation cracking resistance and K_{Ic} are improved, while ν remains almost constant (≈0.29). However, an opposite trend is observed as copper substitute for zinc in zinc borate glasses, possibly because zinc brings more to the mechanical performance than copper thanks to a network tightening effect (C_g is much larger with zinc than with copper (or lead)) while $U_{oZn\text{-}O}$ and $U_{oCu\text{-}O}$ are rather close. The pronounced increase of the optical density (near 400 nm) as the Cu content increases is indicative of an increase of the $Cu^{+} \Leftrightarrow Cu^{2+}$ electron transfer transition especially at CuO content larger than 5 mol%, corresponding to ν values close to 0.3, which is remarkably large for oxide glasses.

6 | CONCLUSION AND PERSPECTIVES

By reviewing the different experimental methods that are currently used to estimate the fracture toughness of glass, we came to the conclusion that the SEPB and CN ones, being self-consistent and well established, should be privileged. In spite of the obvious advantages of indentation-based methods, such as the ease to proceed and the small sample size required, such methods should be avoided inasmuch as possible. Inorganic glasses cover a relatively wide interval of values for γ and K_{Ic}. γ varies from less than 1 J m^{-2} for chalcogenide and borate-rich glasses (with Zn, Pb, and Cu for example), to over 3 J m^{-2} for silicon oxynitride glasses. K_{Ic} is in the 0.2-1.4 MPa·$\sqrt{m}$ interval. A theoretical estimation of γ from the average surface density of atomic bonds on the fracture path and from the relevant bond strengths, and the subsequent calculation of K_{Ic} by means of the elastic properties, is found to predict toughness values in agreement with the experimental ones. This suggests that the experimental toughness data correspond to the crack extension regime and can be viewed as close to the intrinsic values. This corroborates previous observations of crack tips in brittle materials such as glasses and ceramics, which brought to light the atomic sharpness of the crack tip. As a matter of fact, although metallic glasses are disadvantaged by a smaller bond strength (in average), they exhibit much larger toughness due toughening mechanism occurring at the crack initiation stage. In this latter case, measuring the intrinsic toughness still remains challenging. Some guidelines to improve the fracture toughness are proposed, among which playing on the composition in order to (i) reduce the resistance to shear deformation, either by enhancing the atomic packing density (which often leads to an increase in Poisson's ratio), or by lowering T_g (which always lead to an increase of ν measured at ambient temperature), (ii) promote electron mobility (good metals are ductile, and electron hoping can be induced in glasses with multivalent transition metal ions), or (iii) lower the electronegativity mismatch between the host and the major solute elements (especially for metallic glasses). Besides, designing glass-based materials with innovative atomic/molecular organizations, as in phase-separated and nano-crystallized systems, open very promising perspectives.

ACKNOWLEDGMENTS

The European Research Council is greatly acknowledged for the Advanced Grant 320506 (DAMREG) of the 7th framework program "Ideas". The author (S.Y.) would like to thank to the JSPS KAKENHI Grant Numbers 15H04124 and 16K06730.

REFERENCES

1. Lawn BR, Marshall DB. Hardness, toughness and brittleness: an indentation analysis. *J Am Ceram Soc*. 1979;62:347-350.
2. Grenet L. Bull. Soc. Encour. Ind. Natl., Ser. 5, 4, 839 (1999); abridged translation by F.W. Preston. *Glass Ind*. 1934;15:277-280.
3. Freiman SW, Wiederhorn S, Mecholsky JJ. Environmentally enhanced fracture of glass: a historical perspective. *J Am Ceram Soc*. 2009;92:1371-1382.
4. Irwin GR. Analysis of stresses and strains near the end of a crack traversing a plate. *J Appl Mech*. 1957;24:361-364.
5. Evans AG, Charles EA. Fracture toughness determination by indentation. *J Am Ceram Soc*. 1976;59:371-372.
6. Lawn BR, Wilshaw R. Review indentation fracture: principles and applications. *J Mater Sci*. 1975;10:1049-1081.
7. Anstis GR, Chantikul P, Lawn BR, Marshall DB. A critical evaluation of indentation techniques for measuring fracture toughness: I, Direct crack measurements. *J Am Ceram Soc*. 1981;64:533-538.
8. Miyoshi T, Sagawa N, Sassa T. A study on evaluation of K_{Ic} for structural ceramics. *Trans Jpn Soc Mech Eng Ser A*.. 1985;51:2489-2497. (in Japanese).
9. Niihara K. A fracture mechanics analysis of indentation-induced Palmqvist cracks in ceramics. *J Mater Sci Lett*. 1983;2:221-223.
10. Palmqvist S. Method att bestamma segheten hos spread material, sarskit hardmettaler. *Jernkontorets Annaler*. 1957;141:300-307.
11. Niihara K, Morena R, Hasselman DPH. Evaluation of K_{Ic} of brittle solids by the indentation method with low crack-to-indent ratios. *J Mater Sci Lett*. 1982;1:13-16.
12. Glandus JC, Rouxel T, Tai Q. Study of the Y-TZP toughness by an indentation method. *Ceram Inter*. 1991;17:129-135.
13. Ponton CB, Rawlings RD. Vickers indentation fracture toughness test Part 1 Review of literature and formulation of standardized indentation toughness equations. *Mater Sci Tech*. 1989;5:865-872.
14. Yao ZY, Moncke D, Kamitsos EI, et al. Structure and mechanical properties of copper-lead and copper-zinc borate glasses. *J Non-Cryst Sol*. 2016;455:55-68.
15. Sglavo VM, Green DJ. Fatigue limit in fused silica. *J Eur Ceram Soc*. 2001;21:561-567.
16. JIS R 1607. *Testing Methods for Fracture Toughness of High Performance Ceramics*. Tokyo: Japanese Standards Association; 1990.
17. ASTM C 1421-99. *Standard Test Methods for the Determination of Fracture Toughness of Advanced Ceramics at Ambient Temperature. Annual Book Standards, Vol.* ***15.01***. West Conshohocken, PA: ASTM Int.; 1999.
18. ISO 18756. *Fine Ceramics (Advanced Ceramics, Advanced Technical Ceramics) - Determination of Fracture Toughness of Monolithic Ceramics at Room Temperature by Surface Crack in Flexure (SCF) Method*. Geneva: International Organization for Standards; 2003.
19. Petrovic JJ, Jacobson LA, Talty PK, Vasudevan AK. Controlled surface flaws in hot-pressed Si_3N_4. *J Am Ceram Soc*. 1975;58:113-116.
20. Petrovic JJ. Effect of indenter geometry on controlled-surface-flaw fracture toughness. *J Am Ceram Soc*. 1983;66:277-283.
21. Chantikul P, Anstis GR, Lawn BR, Marshall DB. A critical evaluation of indentation techniques for measuring fracture toughness: II, Strength methods. *J Am Ceram Soc*. 1981;64:539-543.
22. Green DJ. *An Introduction to the Mechanical Properties of Ceramics*. Cambridge, UK:Cambridge University Press; 1998:224-231.
23. Aujla JS, Kibble K. Single Edge V-Notch Fractography of Engineering Ceramics. In: Varner JR, Wightman M, eds. *Fractography of Glasses and Ceramics VI*. Hoboken, NJ: A John Wiley & Sons, Inc.; 2012:65-75.
24. ISO 15732. *Fine Ceramics (Advanced Ceramics, Advanced Technical Ceramics) – Test Method for Fracture Toughness at Room Temperature by Single Edge Precracked beam (SEPB) Method*. Geneva: International Organization for Standards; 2003.
25. Nose T, Fujii T. Evaluation of fracture toughness for ceramic materials by a single-edge-precracked-beam method. *J Am Ceram Soc*. 1988;71:328-333.
26. EN 14425-3. *Advanced Technical Ceramics. Test Methods for Determination of Fracture Toughness of Monolithic Ceramics. Part 3: Chevron Notched Beam (CNB) Method*. Brussels: European Committee for Standardization; 2010.
27. ISO 24370. *Fine ceramics (Advanced ceramics, Advanced Technical Ceramics) - Test method for Fracture Toughness of Monolithic Ceramics at Room Temperature by Chevron-Notched Beam (CNB) method*. Geneva: International Organization for Standards; 2005.
28. Munz D, Bubsey RT, Shannon Jr JI. Fracture toughness determination of Al_2O_3 using four-point-bend specimens with straight-through and chevron notches. *J Am Ceram Soc*. 1980;63:300-305.
29. Janssen Ch. Specimen for Fracture Mechanics Studies on Glass. In: Kunugi M, Tashiro M, Soga N, eds. *Proceedings of the 10th International Congress on Glass, Vol. 10*. Tokyo, Japan: Ceramic Society of Japan; 1974:23-30.
30. Yoshida S, Matsuoka J, Soga N. Sub-critical crack growth in sodium germanate glasses. *J Non-Cryst Solids*. 2003;316:28-34.
31. Demetriou MD, Launey ME, Garrett G, et al. A damage-tolerant glass. *Nature Mater*. 2011;10:123-128.
32. Burghard Z, Zimmermann A, Rödel J, Aldinger F, Lawn BR. Crack opening profiles of indentation cracks in normal and anomalous glasses. *Acta Mater*. 2004;52:293-297.
33. Wiederhorn SM, Bolz LH. Stress corrosion and static fatigue of glass. *J Am Ceram Soc*. 1970;53:543-548.
34. Freiman SW, Mulville DR, Mast PW. Crack propagation studies in brittle materials. *J Mater Sci*. 1973;8:1527-1533.
35. Sakaguchi S, Sawaki Y, Abe Y, Kawasaki T. Delayed failure in silica glass. *J Mater Sci*. 1982;17:2878-2886.
36. Evans AG. A method for evaluating the time-dependent failure characteristics of brittle materials – and its application to polycrystalline alumina. *J Mater Sci*. 1972;7:1137-1146.
37. Peter KW. Densification and flow phenomena of glass in indentation experiments. *J Non-Cryst Sol*. 1970;5:103-115.
38. Arora A, Marshall DB, Lawn BR, Swain MV. Indentation deformation/fracture of normal and anomalous glasses. *J Non-Cryst Sol*. 1979;31:415-428.
39. Rouxel T, Ji H, Guin JP, Augereau F, Rufflé B. Indentation deformation mechanism in glass: densification versus shear flow. *J Appl Phys*. 2010;107:094903.
40. Lawn B, Cook RF. Probing material properties with sharp indenters: a retrospective. *J Mater Sci*. 2012;47:1-22.
41. Yoshida S, Sangleboeuf J-C, Rouxel T. Quantitative evaluation of indentation-induced densification in glass. *J Mater Res*. 2005;20:3404-3412.
42. Sellappan P, Rouxel T, Celarie F, Becker E, Houizot P, Conradt R. Composition dependence of indentation deformation and indentation cracking in glass. *Acta Mat*. 2013;61:5949-5965.

43. Rouxel T. Driving force for indentation cracking in glass: composition, pressure and temperature dependence. *Phil Trans R Soc A*. 2015;373:20140140.
44. Scannell GW, Laille D, Célarié F, Huang L, Rouxel T. Interaction between deformation and crack initiation under Vickers indentation in Na_2O-TiO_2-SiO_2 glasses. *Front Mater*. 2017;4:6. https://doi.org/10.3389/fmats.2017.00006.
45. Barlet M, Delaye JM, Charpentier T, et al. Hardness and toughness of sodium borosilicate glasses. *J Non-Cryst Sol*. 2015;417–18:66-79.
46. Januchta K, Yougman RE, Goel A, et al. Structural origin of high crack resistance in sodium aluminoborate glasses. *J Non-Cryst Sol*. 2017;460:54-65.
47. Hermansen C, Matsuoka J, Yoshida S, Yamazaki H, Kato Y, Yue YZ. Densification and plastic deformation under microindentation in silicate glasses and the relation to hardness and crack resistance. *J Non-Cryst Sol*. 2013;364:40-43.
48. Limbach R, Winterstein-Beckmann A, Dellith J, Möncke D, Wondraczek L. Plasticity, crack initiation and defect resistance in alkali-borosilicate glasses: from normal to anomalous behavior. *J Non-Cryst Sol*. 2015;419:97-109.
49. Vullo P, Davis MJ. Comparative study of micro-indentation and Chevron notch fracture toughness measurements of silicate and phosphate glasses. *J Non-Cryst Sol*. 2004;349:180-184.
50. Moysan C, Riedel R, Harshe R, Rouxel T, Augereau F. Mechanical properties of a polysiloxane-derived SiOC glass. *J Eur Ceram Soc*. 2007;27:397-403.
51. Sehgal J, Ito S. Brittleness of glass. *J Non-Cryst Solids*. 1999;253:126-132.
52. Rosales-Sosa GA, Masuno A, Higo Y, Inoue H. Crack-resistant Al_2O_3-SiO_2 glasses. *Scientific Report*. 2016;6:23620. https://doi.org/10.1038/srep23620.
53. Feng G, Qu S, Huang Y, Nix WD. A quantitative analysis for the stress field around an elastoplastic indentation/contact. *J Mater Res*. 2009;24:704-718.
54. Quinn GD, Bradt RC. On the Vickers fracture toughness test. *J Am Ceram Soc*. 2007;90:673-680.
55. Miyazaki H, Hyuga H, Hirao K, Ohji T. Comparaison of fracture resistance as measured by the indentation fracture toughness determined by the single-edge-precracked beam technique using silicon nitrides with different microstructures. *J Eur Ceram Soc*. 2007;27:2347-2354.
56. Yao ZY. Synthesis, structure, and mechanical properties of lead- and zinc-copper borate glasses, Ph-D report. Université de Rennes 1; 2016.
57. Marshall DB, Ratto JJ, Lange FF. Enhanced fracture toughness in layered microcomposites of Ce-ZrO_2 and Al_2O_3. *J Am Ceram Soc*. 1991;74:2979-2987.
58. Sglavo VM, Bosetti P, Trentini E, Ceschini M. Sandwiched-beam procedure for pre-cracking brittle materials. *J Am Ceram Soc*. 1999;82:2269-2272.
59. Trentini E, Kübler J, Sglavo VM. Comparison of the sandwiched beam (SB) and opposite roller loading (ORL) techniques for the pre-cracking of brittle materials. *J Eur Ceram Soc*. 2003;23:1257-1262.
60. Kurkjian CR, Gupta PK, Brow RK, Lower N. The intrinsic strength and fatigue of oxide glasses. *J Non-Cryst Solids*. 2003;316:114-124.
61. Kurkjian CR, Gupta PK, Brow RK. *Int J Appl Glass Sci*. 2010;1:27-37.
62. Mould RE, The Strength of Inorganic Glasses. In: Bonis LJ, Duga JJ, Gilman JJ, eds. *Fundamental Phenomena in the Materials Sciences Vol. 4, Fracture of Metals, Polymers and Glasses*. New York, NY: Plenum; 1967:119-149.
63. Brambilla G, Payne DN. The ultimate strength of glass silica nanowires. *Nano Lett*. 2009;9:831-835.
64. Gupta PK, Kurkjian CR. Intrinsic failure and non-linear elastic behavior of glasses. *J Non-Cryst Solids*. 2005;351:2324-2328.
65. Guerette M, Kurkjian CR, Semjonov S, Huang L. Nonlinear elasticity of silica glass. *J Am Ceram Soc*. 2015;99:841-848.
66. Lower NP, Brow RK, Kurkjian CR. Inert failure studies of sodium silicate glass fibers. *J Non-Cryst Solids*. 2004;349:168-172.
67. Lower NP, Brow RK, Kurkjian CR. Inert failure strains of sodium aluminosilicate glass fibers. *J Non-Cryst Solids*. 2004;344:17-21.
68. Lower NP. Failure studies of glass fibers, Ph-D Dissertation. Rolla, MO: University of Missouri-Rolla; 2004.
69. Ainsworth L. The diamond pyramid hardness of glass in relation to the strength and structure of glass. *J Soc Glass Technol*. 1954;38:479-500.
70. Bartenev GM, Sanditov DS. The strength and some mechanical and thermal characteristics of high-strength glasses. *J Non-Cryst Solids*. 1982;48:405-421.
71. Wang B, Yu Y, Lee YJ, Bauchy M. Intrinsic nano-ductility of glasses: the critical role of composition. *Frontiers Mater*. 2015;2:1-9.
72. Sakka S. Effects of reheating on strength of glass fibers. *Bull Inst Chem Res, Kyoto Univ*. 1956;34:316-320.
73. Lezzi PJ, Evke EE, Aaldenberg EM, Tomozawa M. Surface crystallization and water diffusion of silica glass fibers: causes of mechanical strength degradation. *J Am Ceram Soc*. 2015;98:2411-2421.
74. Yoshida S, Kato M, Yokota A, Sasaki S. Direct observation of indentation deformation and cracking of silicate glasses. *J Mater Res*. 2015;30:2291-2299.
75. Wada M, Furukawa H, Fujita K. Crack resistance of glass on Vickers indentation. *Proc X Int Congr Glass*. 1974;11:39-46.
76. Hagan JT. Micromechanics of crack nucleation during indentations. *J Mater Sci*. 1979;14:2975-2980.
77. Ishikawa H, Shinkai N. Critical load for median crack initiation in Vickers indentation of glasses. *J Am Ceram Soc*. 1982;65:C124-C127.
78. Kato Y, Yamazaki H, Yoshida S, Matsuoka J. Effect of densification on crack initiation under Vickers indentation test. *J Non-Cryst Sol*. 2010;356:1768-1773.
79. Yoshida S, Iwata S, Sugawara T, et al. Elastic and residual stresses around ball indentations on glasses using a micro-photoelastic technique. *J Non-Cryst Solids*. 2012;358:3465-3472.
80. Pezzotti G, Leto A. Contribution to spatially and spectrally resolved cathodoluminescence to crack-tip phenomena in silica glass. *Phys Rev Lett*. 2009;103:175501-175504.
81. Kermouche G, Barthel E, Vandembroucq D, Dubujet P. Mechanical modeling of indentation-induced densification in amorphous silica. *Acta Mater*. 2008;56:3222-3228.

82. Keryvin V, Meng J-X, Gicquel S, et al. Constitutive modeling of the densification process in silica glass under hydrostatic compression. *Acta Mater*. 2014;62:250-257.
83. Rouxel T. Predicting the fracture surface energy and fracture toughness of inorganic glasses. *Scripta Mat*. 2017;137:109-113.
84. Sun KH. Fundamental condition of glass formation. *J Am Ceram Soc*. 1947;30:277-281.
85. Shannon RD. Revised effective ionic radii and systematic studies of interatomic distances in halides and chalcogenides. *Acta Cryst*. 1976;A32:751-767.
86. King SW, Antonelli GA. Simple bond energy approach for non-destructive measurements of the fracture toughness of brittle materials. *Thin Solid Films*. 2007;515:7232-7241.
87. Grüneisen E. *1st rule in "Physical Properties of Solid Materials"*, Zwikker C, eds. New-York, NY: Willey Interscience; 1954, p.90.
88. Makishima A, Mackenzie JD. Calculation of bulk modulus, shear modulus and poisson's ratio of glass. *J Non-Cryst Sol*. 1975;17:147-157.
89. Rouxel T. Elastic properties and short-to-medium range order in glasses. *J Am Ceram Soc*. 2007;90:3019-3039.
90. Rizkalla AS, Jones DW, Sutow EJ. Effect of non-bridging oxygens on the fracture toughness of synthesized glasses. *Ceram Trans J*. 1992;91:12-15.
91. Tuel A, Hommel H, Legrand AP, Kovats E. A Si^{29} NMR study of the silanol population at the surface of derivatized silica. *Langmuir*. 1990;6:770-775.
92. D'Souza AS, Pantano C. Mechanisms for silanol formation on amorphous silica fracture surfaces. *J Am Ceram Soc*. 1999;82:1289-1293.
93. *Handbook of Chemistry and Physics*, Lide DR, eds. 86th edn. Boca Raton, FL: CRC Press, Taylor and Francis Pub; 2005.
94. Wiederhorn SM, Johnson H, Diness AM, Heuer AH. Fracture of glass in vacuum. *J Am Ceram Soc*. 1974;57:336-341.
95. West JK, Hench LL. Silica fracture; Part II A ring opening model via hydrolysis. *J Mater Sci*. 1994;29:5808-5816.
96. Wiederhorn SM. Fracture surface energy of glass. *J Am Ceram Soc*. 1969;52:99-105.
97. Smith DG, Chowdary M. The fracture toughness of slip-cast fused silica. *Mater Sci Eng*. 1975;20:83-88.
98. Vernaz E, Larche F. Effect of a microheterogeneous structure on the fracture toughness of glasses. *J Am Ceram Soc*. 1980;63:286-288.
99. Soga N. Elastic moduli and fracture toughness of glass. *J Non-Cryst Solids*. 1985;73:305-313.
100. Lucas JP, Moody NR, Robinson SL, Hanrock J, Hwang RQ. Determining fracture toughness of vitreous silica glass. *Scripta Met et Mater*. 1995;32:743-748.
101. Schultz RA, Jensen MC, Bradt RC. Single crystal cleavage of brittle materials. *Intern J Fract*. 1994;65:291-312.
102. Mezeix P. Verres et vitrocéramiques du système $BaO\text{-}TiO_2\text{-}SiO_2$: Propriétés mécaniques et couplage électromécanique, Ph-D report. Université de Rennes 1; 2017.
103. Farges F. Coordination of Ti in crystalline and glassy fresnoites: a high resolution XANES spectroscopy study at Ti K-edge. *J Non-Cryst Sol*. 1996;204:53-64.
104. Mezeix P, Célarié F, Houizot P, Gueguen Y, Munoz F, Rouxel T. Elasticity and viscosity of $BaO\text{-}TiO_2\text{-}SiO_2$ glasses in the 0.9 to 1.2Tg temperature interval. *J Non-Cryst Sol*. 2016;445–446:45-52.
105. Reddy KPR, Fontana EH, Helfinstine J. Fracture toughness measurements of glass and ceramic materials using chevron-notched specimens. *J Am Ceram Soc*. 1988;71:C310-C313.
106. Miyata N, Jinno H. Use of Vickers indentation method for evaluation of fracture toughness of phase-separated glasses. *J Non-Cryst Solids*. 1980;38&39:391-396.
107. Shaw RR, Uhlmann DR. Effect of phase separation on the properties of simple glasses. *J Non-Cryst Solids*. 1971;5:237-263.
108. Vernaz E, Larche F, Zarzycki J. Fracture toughness—composition relationship in some binary and ternary glass systems. *J Non-Cryst Sol*. 1980;37:359-365.
109. Shinkai N, Bradt RC, Rindone GE. Elastic moduli and fracture toughness of ternary $PbO\text{-}ZnO\text{-}B_2O_3$ glasses. *J Am Ceram Soc*. 1982;65:123-126.
110. Kato Y, Yamazaki H, Itakura S, Yoshida S, Matsuoka J. Load dependence of densification in glass during Vickers indentation test. *J Ceram Soc Jpn*. 2011;19:110-115.
111. Hirao K, Matsuoka J, Soga N. Inelastic deformation and structure of borate glasses. *J Non-Cryst Solids*. 1989;112:336-340.
112. Hampshire S, Nestor E, Flynn R, et al. Yttrium oxynitride glasses: properties and potential for crystallisation to glass-ceramics. *J Eur Ceram Soc*. 1994;14:261-273.
113. Dériano S, Jarry A, Rouxel T, Sangleboeuf JC, Hampshire S. The indentation fracture toughness (K_c) and its parameters: the case of silica-rich glasses. *J Non-Cryst Sol*. 2004;344:44-50.
114. Sellappan P, Sharafat A, Keryvin V, et al. Elastic properties and surface damage resistance of nitrogen-rich (Ca, Sr)-Si-O-N glasses. *J Non-Cryst Sol*. 2010;356:2120-2126.
115. Rouxel T, Laurent Y. Fracture characteristics of SiC particle reinforced oxynitride glass using chevron-notch three-point bend specimens. *Int J Fract*. 1999;91:83-101.
116. Guin J-P, Rouxel T, Sangleboeuf J-C, Melscoët I, Lucas J. Hardness, toughness and scratchability of Ge-Se chalcogenide glasses. *J Am Ceram Soc*. 2002;85:1545-1552.
117. Guin JP. Comportement mécanique de verres inorganiques : du plus fragile, au plus tenace. . ., Ph-D thesis. Université de Rennes 1; 2001.
118. Boone S, Kleppa OJ. Enthalpies of formation for group IV selenides ($GeSe_2$, $GeSe_2$(am), SnSe, $SnSe_2$, PbSe) by direct-combination drop calorimetry. *Thermochim Acta*. 1992;197:109-121.
119. Shkolnikov EV. Connection between the microhardness and softening temperature and the average atomization enthalpy of chalcogenide glasses. *Sov J Glass Phys Chem*. 1985;11:40-44.
120. Yang G, Gueguen Y, Sangleboeuf J-C, et al. Physical properties of the Ge_xSe_{1-x} glasses in the $0<x<0.42$ range in correlation with their structure. *J Non-Cryst Sol*. 2013;377:54-59.
121. Bauchy M, Wang B, Wang M, et al. Fracture toughness anomalies: viewpoint of topological constraint theory. *Acta Mater*. 2016;121:234-239.
122. Xi XK, Zhao DQ, Pan MX, Wang WH, Wu Y, Lewandowski JJ. Fracture of brittle metallic glasses: brittleness or plasticity. *Phys Rev Lett*. 2005;94:125510.
123. Wang WH. The elastic properties, elastic models and elastic perspectives of metallic glasses. *Progress Mater Sci*. 2012;57:487-656.
124. Gilbert CJ, Ritchie RO, Johnson WL. Fracture toughness and fatigue-crack propagation in a Zr-Ti-Ni-Cu-Be bulk metallic glass. *App Phys Lett*. 1997;71:476-478.

125. Lowhaphandu P, Lewandowski JJ. Fracture toughness and notched toughness of bulk amorphous alloy: Zr-Ti-Ni-Cu-Be. *Scr Mater*. 1998;38:1811-1817.
126. Kawashima A, Kurushita H, Kimura H, Zhang T, Inoue A. Fracture toughness of $Zr_{55}Al_{10}Ni_5Cu_{30}$ bulk metallic glass by 3-point bending testing. *Mater Trans*. 2005;46:1725-1732.
127. Lewandowski JJ, Wang WH, Greer AL. Intrinsic plasticity or brittleness of metallic glasses. *Phil Mag Lett*. 2005;85:77-87.
128. Xu J, Ramamurty U, Ma E. The fracture toughness of bulk metallic glasses. *JOM*. 2010;62:10-18.
129. Seal AK, Chakraborty P, Roy NR, Mukherjee S, Mitra MK, Das GC. Effect of phase separation on the fracture toughness of SiO_2-B_2O_3-Na_2O glass. *Bull Mater Sci*. 2005;28:457-460.
130. Mohajerani A, Zwanziger JW. Mixed alkali effect on Vickers hardness and cracking. *J Non-Cryst Solids*. 2012;358:1474-1479.
131. Wondraczek L, Mauro JC, Eckert J, et al. Towards ultrastrong glasses. *Adv Mater*. 2011;23:4578-4586.
132. Zhang T, Liu F, Pang S, Li R. Ductile Fe-based bulk metallic glass with good soft-magnetic properties. *Mater Trans*. 2007;48:1157-1160.
133. Marsh DM. Plastic flow in glass. *Proc R Soc A Math Phys Sci*. 1964;279:420-435.
134. Magde SV, Louzguine-Luzgin DV, Lewandowski JJ, Greer AL. Toughness, extrinsic effects and Poisson's ratio of bulk metallic glasses. *Acta Mater*. 2012;60:4800-4809.
135. Rouxel T, Yokoyama Y. Elastic properties and atomic bonding character in metallic glasses. *J App Phys*. 2015;118:044901.
136. Greaves GN, Greer AL, Lakes RS, Rouxel T. Poisson's ratio and modern materials. *Nat Mater*. 2011;10:823-837.
137. Miura T, Watanabe T, Benino Y, Komatsu T. Unusual elastic and mechanical behaviors of copper phosphate glasses with different copper valence states. *J Am Ceram Soc*. 2001;84:2401-2408.

How to cite this article: Rouxel T, Yoshida S. The fracture toughness of inorganic glasses. *J Am Ceram Soc*. 2017;00:1–23. https://doi.org/10.1111/jace.15108

Tanguy Rouxel is a Mechanical Engineer (ENSAM, Paris), a Doctor in Ceramic Science (ENSCI, Limoges) and a Professor of Glass Science and Solid Mechanics at the University of Rennes 1. After graduating he became a Post-doctoral Fellow in the Government Industrial Research Institute of Nagoya (then the NIRIN, Japan) for one year and a half. He then held a position as a CNRS Researcher in Ceramics Science for four years. In 1997, he was appointed Professor at the University of Rennes 1, where he founded a laboratory focusing on the study of surface mechanics problems, and flow and fracture in glasses and ceramics. Tanguy Rouxel approach to the mechanical properties of brittle materials, especially glasses, is based on the role of the structure of the material at the atomic and nanoscale levels, and draw knowledges from seemingly disparate fields (chemistry, physics and mechanics) to get insight into the elastic properties, the permanent deformation mechanisms and the surface damages processes. He was awarded - and/or nominated to - the French ceramic society prize (1992), CNRS Bronze medal (1996), the Institute Universitaire de France (2001), the medal of the City of Rennes (2001), the Yvan Peyches Award of the French Academy of Sciences (2007), the Professor Brahm Prakash Visiting Chair, IIS, Bangalore, India (2009), Adjunct Professor of the Chinese Academy of Science, SICCAS, Shanghai, China (2009), the Otto Schott Research Award (2010), and the Advacnced Grant of the European Research Council "Pushing the Frontier of Glass Brittlness" (2012).

Tanguy ROUXEL - tanguy.rouxel@univ-rennes1.fr

Satoshi Yoshida graduated from Kyoto University, Japan, and got a Master degree in Engineering and a Doctor degree in Human and Environmental Studies from Kyoto University. He joined the University of Shiga Prefecture, Japan, in 1995. During the year 2004-2005, he also worked as a visiting professor of the University of Rennes 1, France. Dr. Satoshi Yoshida is currently an associate professor of Department of Materials Science in the University of Shiga Prefecture, Japan. His main research topic is deformation and fracture behaviors of oxide glasses, more specifically residual stress and cracking behaviors of glass under sharp diamond indenters. He also focuses on various properties of glass-forming melts, e.g. the nucleation of bubbles in glass melt. He is also a member of TC06 (Technical committee on the mechanical and nano-mechanical properties of glasses) of ICG (International Commission on Glass), a member of the scientific committee of International Workshop on Flow and Fracture of Advanced Glasses, and a respective member of New Glass Forum, Japan. Dr. Satoshi Yoshida has received the CerSJ awards for advancements in ceramic science and technology (2004), for international exchange encouragement (2009), and for outstanding papers (2011 and 2016) from the Ceramic Society of Japan, and awarded the 14th Otto Schott Research Award (2016) from Ernst Abbe Fund. Satoshi Yoshida – yoshida@mat.usp.ac.jp